

**H19-REGULATED CODING AND NON-CODING RNA
SIGNATURE IN MENINGIOMA:
PREDICTION AND FUNCTIONAL VALIDATION**

A PROJECT REPORT

Submitted as part of B. Tech. Major Project (BB1)

Submitted by:

Khushi Singh

2021BB10332

Guided by:

Prof. Ritu Kulshreshtha



**DEPARTMENT OF BIOCHEMICAL ENGINEERING AND BIOTECHNOLOGY
INDIAN INSTITUTION OF TECHNOLOGY, DELHI**

November, 2024

DECLARATION

I certify that

- a) the work contained in this report is original and has been done by me under the guidance of my supervisor(s).
- b) I have followed the guidelines provided by the Department in preparing the report.
- c) I have conformed to the norms and guidelines given in the Honor Code of Conduct of the Institute.
- d) whenever I have used materials (data, theoretical analysis, figures, and text) from other sources, I have given due credit to them by citing them in the text of the report and giving their details in the references. Further, I have taken permission from the copyright owners of the sources, whenever necessary.

Signed by:
Khushi Singh

CERTIFICATE

It is certified that the work contained in this report titled “H19-regulated Genes and MicroRNAs in Meningioma: prediction and functional validation” is the original work done by Khushi Singh and has been carried out under my supervision.

Signed by:
Prof. Ritu Kulshreshtha

Date:
24.11.24

ABSTRACT

Meningioma is the most common type of intracranial tumour. The World Health Organisation classifies it into 3 grades of malignancy. The intricate histology of meningiomas, combined with the absence of dependable genetic and epigenetic markers, affects the precision of tumour grading, influences disease prognosis, and complicates treatment discussions. Long noncoding RNAs (lncRNAs) may regulate microRNAs (miRNAs) via the competing endogenous RNA (ceRNA) theory. This might further affect the expression of the mRNA targets of these miRNAs.

This project is a subpart of a larger umbrella project in collaboration between AIIMS and IIT Delhi involving total RNA Sequencing of 75 Meningioma patient samples and 4 healthy controls to identify coding and non-coding RNA signatures associated with Meningioma pathogenesis. Previous bioinformatic analysis identified the increase in expression of the long noncoding RNA- H19 to be grade dependent, with highest dysregulation in advanced grade (grade 3). To explore H19-regulated coding and noncoding signatures in meningioma, the 75 patient samples were grouped on the basis of their H19 normalised expression counts relative to median. Differential gene expression analysis reported 222 upregulated and 249 downregulated genes. Comparing these results to established literature (GEO datasets) yielded 15 common upregulated genes (e.g. SOX11, BUB1, KIF11, CCNB2) and 1 common downregulated gene- GPX3. Mirnet 2.0 tool was used to identify the miRNAs that target the upregulated DEGs from which we found the H19 interactors. We used this data to construct an lncRNA-miRNA-mRNA interaction network. We identified hsa-miR-149-5p as an ideal candidate miRNA as it is commonly dysregulated in a variety of cancers and its role has not been studied in meningioma. Interestingly, among the predicted targets of hsa-miR-149-5p, 14 genes (BIRC5, PITX1, RRM2, AURKA, HIST1H2AI, ESPL1, AURKA, BIRC5, CENPF, ESPL1, HIST1H2AI, PITX1, RRM2, TOP2A) were also among the top 20 upregulated hub genes in our data and thus might serve as attractive targets. Overall, our results identified a candidate miRNAs for further analysis and ncRNA-mRNA inter-relationships that may impact meningioma pathogenesis and serve as potent biomarkers and therapeutic targets.

TABLE OF CONTENTS

	Page
Declaration	ii
Certificate	iii
Abstract	iv
Table of Contents	v
List of Tables	viii-ix
List of Figures	x-xi
List of Abbreviations	xii-xiii
Chapter 1: Introduction	1
1.1 Cancer- Burden, Etiology and Classification	1
1.2 Meningioma	2
1.3 Cellular Aberrations in Cancer	3
1.4 Gene Regulation by non Coding RNAs	4
1.5 Objectives	4
Chapter 2: Literature Survey	6
2.1 A review of cancer pathoetiology with a focus on Meningioma	6
2.2 Established Therapeutic Strategies	6
2.3 Role of dysregulated long non-coding RNAs in Meningioma	7
2.4 Role of H19 long non-coding RNA in Cancers	7
2.5 Research Gap	8
Chapter 3: Materials and Methods	9
3.1 AIIMS RNA Sequencing data	9
3.2 Bioinformatics Analyses	9
3.2.1 Differential Gene Expression Analysis	9
3.2.2 Comparative Analysis with Established Gene Dysregulations	9
3.2.3 Gene Ontology Analysis of Differentially Expressed Genes (DEGs)	10
3.2.3.1 Biological Processes	10
3.2.3.2 Molecular Function	10
3.2.3.3 Cellular Components	10

3.2.4 Pathway Analysis of Differentially Expressed Genes	10
3.2.5 Overlap of DEGs with Established Oncogenes and Tumour Suppressor Genes	11
3.2.6 Analysis of Immune Infiltration of tumours	11
3.2.6.1 TIMER Analysis	11
3.2.6.2 ImmReg Comparative Analysis	11
3.2.7 Coexpression Analysis of DEGs with H19 Using cBioPortal Data	12
3.2.8 Protein-Protein Interaction Analysis of Differentially Expressed Genes	12
3.2.9 ceRNA Interaction Analysis for Differentially Expressed Genes	12
3.3 Experimental Validation	13
3.3.1 Primer Design	13
3.3.1.1 Designing Cloning Primers	13
3.3.1.2 Designing Detection Primers	15
3.3.2 Preparation of Overexpression Construct of miR-149	15
3.3.2.1 Temperature Standardisation of Cloning Primers	15
3.3.2.2 PCR Amplification	15
3.3.2.3 Gel Elution	16
3.3.2.4 Restriction Enzyme Digestion	16
3.3.2.5 Ligation	16
3.3.2.6 Transformation	16
3.3.2.7 Validation of presence of miR-149 insert in colonies	16
3.3.2.7.1 Colony PCR	16
3.3.2.7.2 Plasmid Extraction and Digestion	17
3.3.2.7.3 Sequencing	17
3.3.3 Transfection of miR-149 clone in IOMM Lee cell line	17
Chapter 4: Results and Discussion	18
4.1 Bioinformatics Analyses	18
4.1.1 Differentially Expressed Genes	19
4.1.2 Comparison with Literature	23
4.1.3 Gene Ontology Analysis	26
4.1.3.1 Biological Processes	26
4.1.3.2 Molecular Function	26

4.1.3.3 Cellular Components	26
4.1.4 Pathway Analysis	26
4.1.5 Identification of Oncogenes and Tumour Suppressor Genes followed by overlap with meningioma grade 3 associated gene signature	27
4.1.6 Immune Infiltration of Tumours	28
4.1.6.1 TIMER	28
4.1.6.2 ImmReg	29
4.1.7 Coexpression Analysis	32
4.1.8 Protein-Protein Interaction Analysis	34
4.1.9 H19 Associated ceRNA Networks	39
4.1.10 Candidate miRNA Selection	41
4.2 Experimental Validation	42
4.2.1 Primer Design	42
4.2.2 Preparation of Overexpression Construct of miR-149	43
4.2.2.1 Temperature Standardisation of Cloning Primers	43
4.2.2.2 PCR Amplification	45
4.2.2.3 Gel Elution	45
4.2.2.4 Restriction Enzyme Digestion	45
4.2.2.5 Ligation	46
4.2.2.6 Transformation	46
4.2.2.7 Validation of presence of miR-149 insert in colonies	48
4.2.2.7.1 Colony PCR	48
4.2.2.7.2 Plasmid Extraction and Digestion	49
4.2.2.7.3 Sequencing	50
4.2.3 Transfection of miR-149 clone in IOMM Lee cell line	50
Chapter 5: Summary and Conclusions	51
References	52
Supplementary	55

LIST OF TABLES

Table No.	Title	Page No.
4.1	Analysis of AIIMS dataset classified on the basis of H19 counts	25
4.2	List of top 20 significant differentially expressed genes obtained after analysis in R	27
4.3	Transcription Factors and Ribosome Binding Proteins common to both DEGs and ImmReg data	35
4.4	DEGs predicted to be coexpressed with the H19 long non-coding RNA	38
4.5	Top 20 hub genes from upregulated genes	41
4.6	Top 20 hub genes from downregulated genes	43
4.7	miRNAs found common to H19+DEG interactors and AIIMS dysregulated miRNA lists	46
4.8	Details of cloning and detection primers for hsa-miR-149-5p	48
4.9	Nanodrop analysis of DNA eluted from gel	51
	Supplementary Tables	
S1	Top 20 biological processes significantly enriched in association with upregulated DEGs	60
S2	Biological processes significantly enriched in association with downregulated DEGs	62
S3	Molecular functions the products of the upregulated DEGs are implicated in	62
S4	Molecular functions the products of the downregulated DEGs are implicated in	63
S5	Cellular components overrepresented in association with upregulated DEGs	63

S6	Cellular components overrepresented in association with downregulated DEGs	66
S7	Pathways in which the upregulated DEGs are significantly implicated.	67
S8	Pathways in which the downregulated DEGs are significantly implicated.	67

LIST OF FIGURES

Fig. No.	Title	Page No.
1.1	Subclassification of Meningioma on the basis of location of tumour in the brain	2
3.1	miR-149-5p precursor sequence from miRbase	13
3.2	gene sequence of miR-149 from Ensembl	14
3.3	Primer design in gene runner, the pink region represents the miR-149 precursor sequence	15
3.4	pcDNA 3.1 (+) vector	16
3.5	Forward primer	17
3.6	Reverse Primer	18
3.7	Results of UCSC in silico PCR	19
3.8	Thermo double digest calculator for Tango Buffer	20
4.1	Proportion of cases of high and low H19 counts across parameters in the AIIMS dataset	24
4.2	Volcano plot showing significant ($p\text{adj} < 0.05$, blue) and significant + $ \log_2 \text{fold change} > 1$ (red) genes from the differential gene expression analysis result.	26
4.3	Comparison of differentially expressed genes with GEO datasets	29
4.4	Gene Ontology analysis for Upregulated genes	30
4.5	Gene Ontology analysis for Downregulated genes	30
4.6	Pathways in which the upregulated DEGs are significantly implicated.	32

4.7	Common Oncogenes and Tumour Suppressor genes amongst our Differentially Expressed genes and known cancer related genes from oncoKB	33
4.8	Significantly different immune cell infiltration in samples based on H19 count	34
4.9	Complete network obtained from PPI of upregulated genes	39
4.10	First cluster obtained from PPI of upregulated genes	40
4.11	Top 20 hub genes from upregulated genes	40
4.12	Complete network obtained from PPI of upregulated genes	42
4.13	First cluster obtained from PPI of downregulated genes	42
4.14	Top 20 hub genes from downregulated genes	43
4.15	lncRNA-miRNA-mRNA interaction network	45
4.16	Target sequence of miR-149-5p in H19 from StarBase	47
4.17	All Ensembl transcripts except H19-211, 217, 221 and 223 contain the target sequence	47
4.18	PCR amplification results at different temperatures	50
4.19	Agarose gel analysis of restriction enzyme digestion	52
4.20	Colonies obtained after transformation with pcDNA 3.1+ and miR-149 ligation mixtures	53
4.21	Results of colony PCR	54
4.22	Results of restriction digestion of plasmids extracted from colonies chosen after colony PCR.	55

LIST OF ABBREVIATIONS

S. No.	Abbreviation	Full Form
1.	DNA	Deoxyribonucleic acid
2.	RNA	Ribonucleic Acid
3.	mRNA	Messenger RNA
4.	ncRNA	Non-coding RNA
5.	tRNA	Transfer RNA
6.	rRNA	Ribosomal RNA
7.	siRNA	Small interfering RNA
8.	lncRNA	Long non-coding RNA
9.	miRNA	Micro RNA
10.	MRE	miRNA recognition elements
11.	ceRNA	Competing endogenous RNA
12.	GBM	Glioblastoma
13.	NCI	National Cancer Institute
14.	NIH	National Institute of Health
15.	CNS	Central Nervous System
16.	RT-qPCR	Reverse Transcriptase quantitative Polymerase Chain Reaction
17.	RIP	RNA Immunoprecipitation
18.	AIIMS	All India Institute of Medical Sciences

19.	GEO	Gene Expression Omnibus
20.	DEGs	Differentially expressed genes
21.	KEGG	Kyoto Encyclopedia of Genes and Genomes
22.	MSKCC	Memorial Sloan Kettering Cancer Center
23.	TSGs	Tumour suppressor genes
24.	TIMER	Tumour Immune Estimation Resource
25.	ImmReg	The Regulon Atlas of Immune-related Pathways across Cancer Types
26.	TFs	Transcription Factors
27.	RBPs	Ribosome Binding Proteins
28.	PPI	Protein-protein interaction
29.	STRING	Search Tool for Retrieval of Interacting Genes
30.	CLIP seq	Cross-linking immunoprecipitation + sequencing
31.	UCSC	University of California, Santa Cruz

Chapter 1

Introduction

Cancer is a devastating human disease. It is characterised by uncontrolled cell division of mutant cells, which may arise from almost anywhere among the approximately 30 trillion cells in the human body. It is a global phenomenon, with millions of new cases diagnosed each year worldwide. The most dangerous ability of cancer cells is their rapid proliferation and ability to invade nearby tissues and spread throughout the body. It is one of the leading causes of death at an international level, and has been an active area of research for decades. While our understanding of this often fatal disease has been greatly enhanced, a complete cure for cancer is known till date. Research in this field aims to further explore the genetic aberrations underlying cancer, with the hope of developing better diagnostic tools and therapies.

1.1 Cancer- Burden, Etiology and Classification

The World Health Organisation lists cancer as one of the top 10 causes of death around the world.¹ The year 2022 saw approximately 20 million new incidents of cancer, and 9.7 million cancer-related deaths worldwide. The National Cancer Institute (NCI), National Institute of Health (NIH), USA predicts that in 2024 alone, 2 million new cases of cancer will be diagnosed in the United States, of which 0.6 million will be fatal, with these numbers rising to 29.9 million new cases and 15.3 million deaths by 2040².

The underlying cause of cancer is genetic mutations. These may be inherited, result from erroneous DNA replication or be caused by carcinogens in our surroundings. Cancer initiates as a few mutant cells, with damaged cellular replication machinery, which proliferate rapidly and may form lumps of tissues called tumours. These tumours, if malignant, may invade surrounding tissues (metastasis) leading to the spread of cancer within the patient's body. Cancerous cells replicate even in the absence of the 'growth signal', ignore signals for apoptosis (programmed cell death), promote growth of blood cells towards tumours and avoid/hijack the immune system. Cancer cells are often heavily mutated, with numerous chromosomal insertions and deletions. This may result in different nutritional needs and energy generation pathways. These

distinctions between regular and cancerous cells contribute to the pathogeny of the disease, but also serve as key targets for many anti-cancer therapies.

There are over a 100 known types of cancers. They are generally classified on the basis of where they occur in the body, but can also be categorised on the basis of the type of mutant cell. Cancers are ranked by grade, which is established by the amount of phenotypic differences observed when viewing a normal cell vs a post-biopsy cancer cell under a microscope. Higher differentiation between the cells denotes a higher grade of cancer. The extent of cancer in a patient is characterised by stage, which depends on the size of the tumour at diagnosis and whether or not it is metastasizing.

1.2 Meningioma

Meningioma is the most common type of primary Central Nervous System (CNS) tumour, accounting for approximately 37.6% of them. These tumours are so called because they originate in the meninges - the layers of tissue cushioning the brain and the spinal cord. Meningiomas are further subclassified into Convexity, Falcine, Intraventricular, Skull base, Sphenoid wing, Olfactory Groove, Posterior fossa and Suprasellar meningioma on the basis of the location of the tumour in the brain.

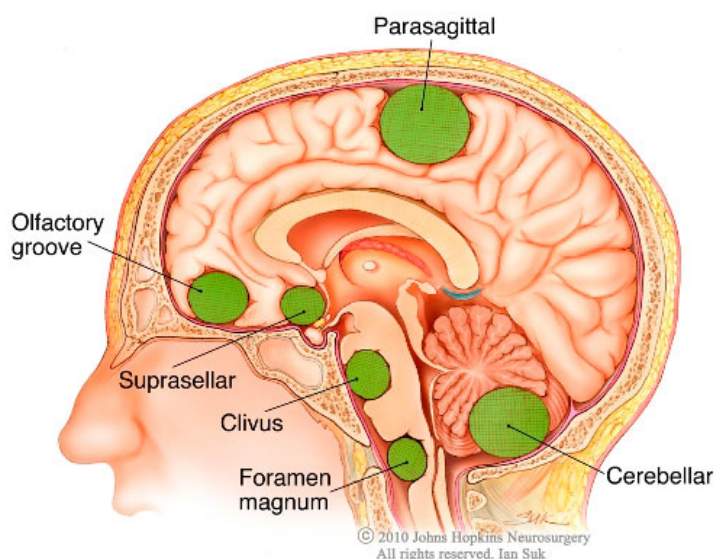


Figure 1.1 Subclassification of Meningioma on the basis of location of tumour in the brain

Johns Hopkins Neurosurgery, 2010

Tumours can be classified into recurrent and non-recurrent based on the tumour's ability to re-establish itself after a period of remission. Meningiomas are graded from 1 to 3 on the basis of tumour tissue analysis. Grade 1 tumours are the most prevalent, constituting 80-81% of all Meningioma cases³. They are benign and they proliferate slowly. However, 1 to 3% become malignant with a 5-year survival rate of 32 to 64%. Grade 3 Meningiomas are rare, 1.7%, but they are malignant, proliferate fast and have high recurrence rates. Meningioma disproportionately affects adults, with an incidence of 75.5/100,000 in the 75-84 age bracket, in comparison to children, 0.14/100,000 in the 0-19 age bracket. The exact cause of Meningioma is unknown, but some known risk factors are genetic disorders, hormonal therapy, exposure to radiation, type 2 Neurofibromatosis and family history.⁴ Most meningioma patients are asymptomatic, but symptomatic patients usually require surgery to remove the tumour. The estimated survival over 10 years for meningioma is 57.1 and 77.7% (for patients diagnosed at 20–44 years.)³

1.3 Cellular Aberrations in Cancer

The onset of cancer depends on a wide range of genetic and chromosomal alterations that contribute to tumorigenesis and cancer progression. The genetic dysregulations underlying cancers play critical roles in specific cancers by directly interacting with or indirectly, after downstream processing, regulating oncogenes and tumour suppressor genes. These alterations facilitate uncontrolled cell division and may also impact other cellular processes, including metabolism and immune evasion.

One of the most important indirect contributions of these aberrations to the pathoetiology of cancer is the alteration of immunologic signalling pathways, enabling cancer cells to escape immune surveillance. For instance, genetic and epigenetic changes in oncogenic signalling pathways, like RAS-MAPK and PI3K-AKT-mTOR, can disrupt interferon signalling and antigen processing, making it difficult for immune cells to recognize and attack tumour cells effectively⁵. Cancer cells may also exploit immune checkpoint pathways to inhibit T cell activation, thereby preventing an effective immune response and indirectly promoting tumorigenesis.

1.4 Gene Regulation by non Coding RNAs

More than 93% of the human genome is transcribed into RNA, but only 2% is translated into mRNA which is translated into proteins.⁶ The remaining 91% of the transcribed genome consists of non-coding RNAs (ncRNAs), ribonucleic acids that do not code for proteins. Instead, these ncRNAs play crucial roles in gene regulation. They can be divided into various types- transfer RNAs (tRNAs), ribosomal RNAs (rRNAs), and smaller regulatory RNAs like microRNAs (miRNAs), small interfering RNAs (siRNAs), and long non-coding RNAs (lncRNAs). These ncRNAs have multiple regulatory roles like chromatin remodelling, transcriptional regulation, and post-transcriptional modifications and influence gene expression at various levels. Their dysregulation has been linked to various diseases, including cancer, where they can act as oncogenes or tumour suppressors by modulating the activity of target genes. This modulation can be explained by the competing endogenous RNAs (ceRNAs) hypothesis, which proposes that various RNA molecules- mRNAs, lncRNAs etc. can regulate each other by competing for shared miRNAs.⁷ These RNAs contain miRNA recognition elements (MREs) that allow them to bind to the same miRNAs, effectively causing the lncRNAs to act as "sponges" that sequester the miRNAs and prevent them from binding to their target mRNAs. For example, if an lncRNA acts as a ceRNA and sponges a miRNA, it reduces the availability of that free miRNA. The free miRNA would normally bind to mRNAs and reduce their expression. But the presence of the lncRNA reduces the availability of the interacting miRNA and indirectly increases the expression of the mRNAs usually targeted by that miRNA. Dysregulation of ceRNA networks has been heavily implicated in cancer.⁸

1.5 Objectives

The current project is a subpart of a larger umbrella project in collaboration between AIIMS and IIT Delhi involving total RNA Sequencing of 75 Meningioma patient samples and 4 healthy controls to identify coding and non-coding RNA signatures associated with Meningioma pathogenesis. Previous bioinformatic analysis identified the long noncoding RNA H19 as the most dysregulated lncRNA across all three Meningioma grades w.r.t controls. In this project, the 75 patient samples, previously part of the study, were characterised into “high H19” and “low H19” groups on the basis of their normalised expression counts relative to median. The raw

counts of mRNAs previously identified in the study were analysed for differential expression between high and low H19 groups. This project has three key objectives:

1) Derivation of H19-associated gene signatures in Meningioma

- Differential gene expression analysis of mRNA counts across the high and low H19 patient groups.
- Gene Ontology analysis (Enrichr) for biological processes, molecular function and cellular components; pathway analysis (KEGG); analysis to identify oncogenes and tumour suppressor genes (oncoKB); analysis of immune infiltration of tumours (TIMER 2.0, ImmReg), coexpression analysis (cBioPortal), protein-protein interaction analysis (STRING, Cytoscape)

2) To study the H19 associated ceRNA networks in meningioma

- Plotting H19 interaction network in Cytoscape

3) Experimental validation of H19 regulated genes/miRNAs in Meningioma

- Target gene/miRNA transcripts quantification via RT-qPCR and Western blotting post H19 expression modulation.
- Validation of H19-target interactions via techniques such as Dual luciferase assay and RNA-Immunoprecipitation (RIP).

4) Functional validation of key genes/miRNAs in meningioma through cell-based assays

- Investigation of effect of candidate H19-regulated gene/microRNA on cancer hallmarks like proliferation, migration and apoptosis

Chapter 2

Literature Survey

2.1 A review of cancer pathoetiology with a focus on Meningioma

Meningiomas usually originate from meningotheelial arachnoid cap cells.⁴ Most of them are sporadic and benign with low rates of proliferation. They exhibit one or more focal chromosomal deletions and this number increases as they turn malignant, which is accompanied by faster proliferation and classified as higher grade Meningiomas. Genetic alterations are found in up to 60% of sporadic meningiomas. A genetic mutation on chromosome 22 in neurofibromatosis type 2 is one of the most common predisposing conditions seen in sporadic meningiomas. Other chromosomal mutations reported are 1p, 6q, 14q, and 18q.⁴ Hormonal influences, especially progesterone and its receptor, have been implicated in the development and growth of meningiomas, especially in females accounting for the higher prevalence of female patients. Over 70% of meningiomas are positive for progesterone receptors.⁹ Environmental factors, like exposure to ionising radiation, have also been associated with an increased risk of meningioma.

Meningiomas are divided into 3 grades. Grade 1 meningiomas comprise over 80% of the cases. They lack anaplastic features seen in other grades. A histopathological characteristic of meningiomas is the growth of meningotheelial cells that mineralize into psammoma bodies. Sometimes hyperostosis of the bone adjacent to the tumour is identifiable. Grade 2 meningiomas are atypical lesions which show brain invasion. They are characterised by at least 3 of: necrosis, sheet-like growth, prominent nuclei, increased cellularity and high nucleus/cytoplasm ratio. They may also be indicated by increased mitotic activity (4-19 mitoses per 10 high-power fields).¹⁰ Grade 3 Meningiomas are anaplastic, malignant lesions with a high rate of distant metastases. They exhibit very high mitotic activity (20 or more mitoses per 10 high-power fields).

2.2 Established Therapeutic Strategies

Therapeutic strategies in cancer are largely dependent on the tumour's characteristics and location as well as the patient's medical history. Meningioma prognosis and treatment strategies

are also dependent on the tumour microenvironment, comprising immune cells, endothelial cells, extracellular matrix components, etc. The primary treatment modality is surgical resection with the aim of complete removal of the lesion and affected tissue.¹¹ Technological advances have been made to minimise the invasiveness of this method. However, surgery may be infeasible due to the tumour's proximity to critical neurovascular structures. In such cases, adjuvant radiation therapy - including external beam radiation and stereotactic radiosurgery - may be recommended. For atypical and anaplastic meningiomas, which exhibit recurrence, chemotherapy is being explored as a potential treatment, but is not yet completely established.¹² Active surveillance is suggested for asymptomatic patients with high surgical risks. Therapies targeting specific molecular pathways dysregulated in Meningioma are an emerging area of research.

2.3 Role of dysregulated long non-coding RNAs

Dysregulated long non-coding RNAs (lncRNAs) are implicated to play a central role in cancer pathogenesis due to their influence on the various hallmarks of cancer like cell proliferation, apoptosis, and metastasis. lncRNAs are ribonucleic acid molecules over 200 bp in length that do not code for proteins. They can enhance or suppress cancers depending on their interaction networks with microRNAs (miRNAs) and messenger RNAs (mRNAs). Many lncRNAs have been implicated in Meningioma.¹³ These lncRNAs behave as competitive endogenous RNAs (ceRNAs) and sequestering microRNAs that interact with oncogenic or tumour-suppressive mRNAs, thus contributing to cancer prognosis.

2.4 Role of H19 long non-coding RNA in Cancers

The long non-coding RNA (lncRNA) H19, located on chromosome 11p15.5, is established as a crucial oncogenic regulator in various cancers.¹⁴ It is reported to be upregulated in breast, ovarian, and gastric cancers, where it contributes to tumorigenesis and progression by promoting cell proliferation, invasion, and metastasis. H19 functions primarily as a competitive endogenous RNA (ceRNA), by sponging microRNAs and thereby modulating the expression of target mRNAs. H19 has also been implicated in epithelial-mesenchymal transition (EMT), a key process for metastasis, by downregulating E-cadherin expression through its interactions with various molecular partners.¹⁵ Aberrant H19 expression has also been associated with chemoresistance.¹⁶ The role of H19 lncRNA in Meningioma has not been extensively studied.

However, a 2023 study exploring the H19/miR-483-5p/IGF-2 axis discovered that the inhibition of this pathway leads to a rapid loss in Meningioma tumour cell viability.¹⁷

2.5 Research Gap

Despite decades of research, no complete cure for Meningioma is known. The benign cases are usually treated by invasive surgical methods, while the therapies for higher grades are less established. Given the heavy burden of the disease, a cure for Meningioma is the need of the hour. Despite the known multifaceted roles the H19 lncRNA plays in other cancers, and its promising role as a marker for diagnosis and prognosis as well as a drug target for therapy, its role has not been extensively studied in the context of Meningioma. Hence, this project, titled “H19 regulated coding and non-coding RNA signature in Meningioma: prediction and functional validation” aims to bridge this research gap and explore the role of the upregulated lncRNA H19 in the prognosis of Meningioma with a focus on its ceRNA interaction networks that contribute to the pathogenesis of cancer, with the ultimate goal of finding a therapeutic target to cure Meningioma.

Chapter 3

Materials and Methods

3.1 AIIMS RNA Sequencing data

RNA Sequencing data was obtained from the All India Institute of Medical Sciences (AIIMS) for (N=75) Meningioma patient samples and (N=4) controls. Raw and normalised noncoding RNA and mRNA counts were available, along with a list of the miRNAs found dysregulated. Additional information about the patients, including biographical data, grade of cancer, recurrence status etc. was provided. Based on prior bioinformatic analysis in the lab, we have a working hypothesis suggesting that the dysregulation of H19 may be critical to the pathoetiology of Meningioma.

3.2 Bioinformatics Analyses

The AIIMS data was used to perform thorough bioinformatic analyses from different perspectives to obtain a comprehensive picture of the observed gene dysregulations in the patient samples.

3.2.1 Differential Gene Expression Analysis

The patients in the AIIMS dataset were classified into having high or low counts of the long noncoding RNA H19, on the basis of the median H19 count- 201.99, observed in the sample. The samples were arranged in the order of increasing H19 counts to analyse differential gene expression in samples with high H19 counts vs samples with low H19 counts, using their mRNA counts. This analysis was performed in R using the DeSeq2 package¹⁸. The obtained list of dysregulated genes was subjected to cutoffs to ensure significance. Only entries with an adjusted p-value < 0.05 and absolute log 2 fold change > 1 were retained.

3.2.2 Comparative Analysis with Established Gene Dysregulations

The list of dysregulated genes between high and low H19 groups was compared to differentially expressed genes identified between grade 3 vs grade 1 and recurrent vs non-recurrent meningioma from 6 publicly available Gene Expression Omnibus (GEO)¹⁹ datasets: GSE16181, GSE16581, GSE43290, GSE74383, GSE101638 and GSE183653. This comparative analysis

was performed to validate our preliminary result by noting overlaps of our differentially expressed genes (DEGs) with the datasets.

3.2.3 Gene Ontology Analysis of Differentially Expressed Genes (DEGs)

Gene ontology analysis was performed to interpret and analyse the functions of the DEGs and their roles in various biological processes. The tool “Enrichr” was used to carry out this analysis. Enrichr is a powerful web-based tool for gene set enrichment analysis, allowing for interpretation and analysis of biological data derived from genomic studies²⁰. It also serves as a gene set search engine, enabling querying of large libraries of annotated gene sets to identify significant associations with input gene lists.

3.2.3.1 Biological Processes

The DEGs were analysed for their involvement in the biological processes in the cell to establish which, if any, were enriched. This analysis was performed separately for upregulated and downregulated genes.

3.2.3.2 Molecular Function

The elemental activities of the DEG products at the molecular level, such as binding, catalysis etc. were assessed by noting differences in molecular function. This analysis was performed separately for upregulated and downregulated genes.

3.2.3.3 Cellular Components

Cellular components were analysed to understand the locations in the cell that were most affected by the DEG products. Upregulated and downregulated genes were analysed separately.

3.2.4 Pathway Analysis of Differentially Expressed Genes

Pathway analysis was performed using the Kyoto Encyclopedia of Genes and Genomes (KEGG)²¹. It is a comprehensive database resource that integrates various biological data to facilitate the understanding of biological systems at multiple levels. Separate analyses were conducted for up and downregulated DEGs.

3.2.5 Overlap of DEGs with Established Oncogenes and Tumour Suppressor Genes

Data from the oncoKB database was used to establish which DEGs have been implicated in cancer. OncoKB is a precision oncology knowledge base developed by Memorial Sloan Kettering Cancer Center (MSKCC). It is recognised by the FDA and provides comprehensive information about somatic mutations in cancer. It serves as an essential clinical decision support tool, offering detailed, evidence-based insights into the biological and clinical implications of over 5,000 cancer gene alterations. The list of final DEGs from high vs low H19 counts of patient samples was intersected with the one from Grade 3 Meningioma vs control. This intersection was then compared to the oncogenes obtained from oncoKB. This procedure was repeated to obtain tumour suppressor genes (TSGs) in our list of DEGs.

3.2.6 Role of Differentially Expressed Genes in Immune Infiltration of tumours

Tumours formed in cancer trigger an immune response. The presence and types of immune cells infiltrating a tumour can significantly influence tumour behaviour and patient outcomes. Immune cell infiltration also gives a better idea about the tumour microenvironment. The DEGs were tested for genes corresponding to this immune infiltration using two tools: TIMER and ImmReg.

3.2.6.1 TIMER Analysis

TIMER stands for Tumour Immune Estimation Resource. It is a web-based tool designed for the systematic analysis of immune cell infiltration in various types of cancer. TIMER 2.0 was used for this analysis. It utilises six state-of-the-art algorithms for immune deconvolution: TIMER, xCell, MCP-counter, CIBERSORT, EPICand quanTIseq. We submitted our DEG list to TIMER and downloaded the results. These results were then analysed for significance using a Python script.

3.2.6.2 ImmReg Comparative Analysis

ImmReg - The Regulon Atlas of Immune-related Pathways across Cancer Types- is a digital platform designed to manage and visualise immune-related pathways across various cancer types. It serves as a regulon atlas, focusing on the regulation of immune system genes and their perturbations, which are significant in the development of different cancers. We obtained their data on the Transcription Factors (TFs) and Ribosome Binding Proteins (RBPs) implicated in

cancers and their associated immune cells and pathways. This list was then intersected with our DEGs.

3.2.7 Coexpression Analysis of DEGs with H19 Using cBioPortal Data

Coexpression analysis was used to identify genes that exhibit similar expression patterns across the samples. It was undertaken with the aim of understanding the functional relationships between genes, as coexpressed genes are often involved in the same biological processes or regulatory pathways. cBioPortal, an open-access, open-source platform for interactive exploration and analysis of large-scale cancer genomics data sets, was used to perform this analysis.

3.2.8 Protein-Protein Interaction (PPI) Analysis of Differentially Expressed Genes

Protein-protein interaction (PPI) analysis was undertaken to study the interactions between proteins, the products of our DEGs, and understand their roles in various biological processes and cellular functions. These interactions are crucial because most cellular activities are mediated by protein complexes, and understanding how proteins interact can provide insights into cellular mechanisms, disease pathways, and potential therapeutic targets. This analysis was performed using STRING (Search Tool for Retrieval of Interacting Genes), a comprehensive database and web-based tool, which integrates known and predicted PPIs from various sources. Upregulated and downregulated DEGs were analysed separately. The STRING mapping generated was then exported to Cytoscape for further analysis and better visualisation.

3.2.9 ceRNA Interaction Analysis for Differentially Expressed Genes

Competing endogenous RNAs (ceRNAs) are a class of RNA molecules that regulate each other by competing for shared microRNAs (miRNAs). This regulatory mechanism suggests that various RNA types, including messenger RNAs (mRNAs), long non-coding RNAs (lncRNAs), and pseudogenes, can influence each other's expression levels through their miRNA response elements (MREs). The ceRNA analysis was performed using Mirnet 2.0, a comprehensive biological database that serves as the primary repository for microRNA (miRNA) sequences and annotations. The list of DEGs was uploaded to Mirnet 2.0 to obtain the list of all miRNAs that interact with our differentially expressed mRNAs. This miRNA list was then re-uploaded to

MirBase to get the lncRNAs interacting with the miRNAs that interact with our DEGs. The list of lncRNAs was then filtered for only H19 interactors, thus leaving us with a list of miRNAs that interact with both- the DEGs and our lncRNA of interest- H19. This miRNA list was then intersected with the list of dysregulated miRNA from AIIMS.

3.3 Experimental Validation

3.3.1 Primer Design

The bioinformatics analyses undertaken in section 3.2 suggests the downregulated miRNA hsa-mir-149-5p as an excellent candidate which may play a key role in Meningioma. hsa-miR-149-5p (MIMAT0000450; precursor- MI0000478) was also found to bind to H19 via using miRNet 2.0 (using ENCORI/starBase as default software). Indirect CLIP Seq data was cited as evidence, no Ago experiment was directly performed in humans but the interaction has been proven in rats.²² In the first step of experimental validation, we wanted to clone miR-149 precursor sequence to exogenously overexpress this miRNA in IOMM Lee cells. Further, we aim to functionally characterise this microRNA in meningioma using the above clone.

3.3.1.1 Designing Cloning Primers

The miR-149-5p precursor sequence was identified from miRbase (Fig 3.1)



Fig 3.1: miR-149-5p precursor sequence from miRbase

Now, the gene sequence of miR-149 was obtained from Ensembl. The precursor sequence from miRbase was matched to the Ensembl gene sequence. Then, the region 200 bp up and downstream of this precursor region was chosen for cloning (Fig 3.2).

Gene: MIR149 ENSG00000207611

Description	microRNA 149 [Source:HGNC Symbol;Acc: HGNC:31536]
Gene Synonyms	HSA-MIR-149, MIRN149
Location	Chromosome 2: 240,456,001-240,456,089 forward strand. GRCh38:CM000664.2
About this gene	This gene has 1 transcript (splice variant).
Transcripts	Show transcript table

Marked-up sequence ?

[Download sequence](#) [BLAST this sequence](#)

Exons MIR149 exons All exons in this region

Markup loaded

```
>chromosome:GRCh38:2:240455401:240456689:1
CTTGACCTGAGCACGCCAGGGCCAGGGGAGGGGGGGGGGGGGGGAGGGGCCAGATGCCCTC
CTGCACGGGGGGAGGGATGGGCTGCCGGACTCACCCCTAGGTGGAAAATGCCCTC
CCTCTGGGTGGAGGGAGAGAAAGCCAGGAAGGGAGAGGGAGGGACATGGGGAGGGTT
CCCCCTGGGCTTGGAGCTTATCCCCAGGTGGTGGAGCTGAGAGAAGTGGTGGGGAGG
CCCCCTGGGGTGGGGAGGCCCTGGGGGGGGATTAAAGATGACAGCTGGCTTGGGCA
CATTGCTCTCATTAGAAAGGCCAGCCCCTGGCATTCTTCAGGAGGGGGCTTGGCTT
TGCCGGCGCTCAGGGGACTCTGAGAGCCGGCCTCTCCCATCTCATGTCAGGACACA
ACCTGTGGCCCCGGCCCTGCGCCGGGGAGCTCCGCAGAAAGGAGCCAGCGGGAGGCCT
CTGCCCTTIGACTGCGTGCCTCACGCCAGCGGGCCCTAGGGGGCCGCTGATCCA
GCCCTGGGGAGGGCTTCCAGGGCCTTGGCTCCAGCCTGCCAGGGGGCTCCAG
GCCCGCAGGGGAGCTCTGGCTCCCTGTCTTCACTCCCTGCTTGCCAGGGAGGGAGG
GGGACGGGGCTGTGCTGGGCACTTGAACAACGGCAGTCGCCGGGGCTGGCGAG
TTGGCCGGGGGGCTGAGGGGTGGGGGGAGGGCTGAGGGCCGGGGGGGGGGCTGGCGGG
CCGTGAGGGGGTGTGAGAGGGTGGCTGACGGCGCCAGGGAGGCCCTCAAGAACCTGCAAGGT
GGGGGAGCTCCCATATCTTACGGGTGTTTGGGCTCACCTCTCATGCTCTGTCAGC
CTCTCCCGTCTGGCTGGTGGGGCTGGGGAGTGGTCCGCCGGACCTGCCAGGGAGGG
GCACAGGGAGGCCAGGGGGAGGCCACCCACCCCTCTCCCTAGGAATGCTTGAACCT
AGTCTCTGAGTCTTGGACCACTCTCGTGTGCTGGCCAGCCAGCTGGCTGGGGTG
CCCCGTCACAGCTGAGCCCCTCTCAGCTGAGCCCAGGGTGTGTACCGGGAGCTCAGCT
GGCACCTGGCACCCCTGGGAGCCAGCAGTCTCCCTCCACTGCCAGCCATTACCATC
ATGTGTCGGCTGACCTGTGCTCTGGTGGGAGCCCTGGGAGGGTGCACAGGGCCC
CATCACAGCCCACACCTCGAGAGACGC
```

Fig 3.2: gene sequence of miR-149 from Ensembl

Precursor sequence of miR-149

5' GCCGGCGCCGAGCTCTGGCTCCGTGTCTTCACTCCGTGCTTGCCAGGGAGGG
AGGGAGGGACGGGGCTGTGCTGGGGCAGCTGGA 3'

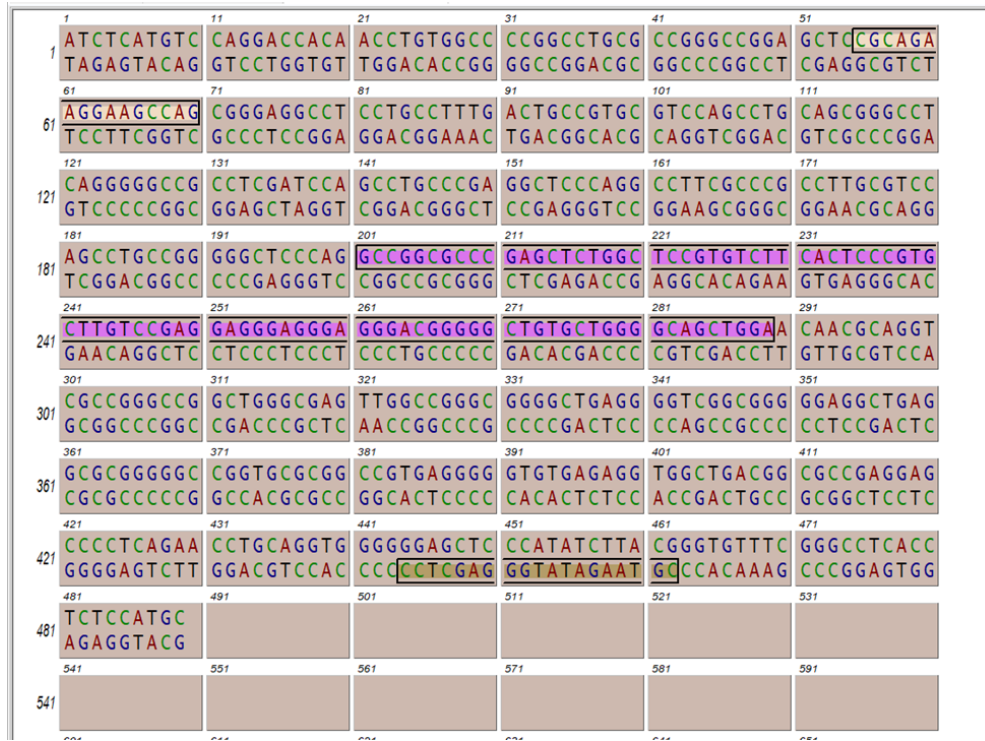


Fig 3.3: Primer design in gene runner, the pink region represents the miR-149 precursor sequence

Then primers were designed keeping in mind all rules (length, GC%, ability to form homo- and hetero-dimers, specificity, absence of secondary structures, melting temperature; images attached). The forward primer is highlighted in white while reverse primer is highlighted in mustard (Fig 3.3).

The plasmid chosen for cloning was pcDNA 3.1 (+) which is preferred for mammalian cells due to its strong CMV promoter, to achieve desired expression of target gene. It is a 5428 bp long plasmid (Fig 3.4).

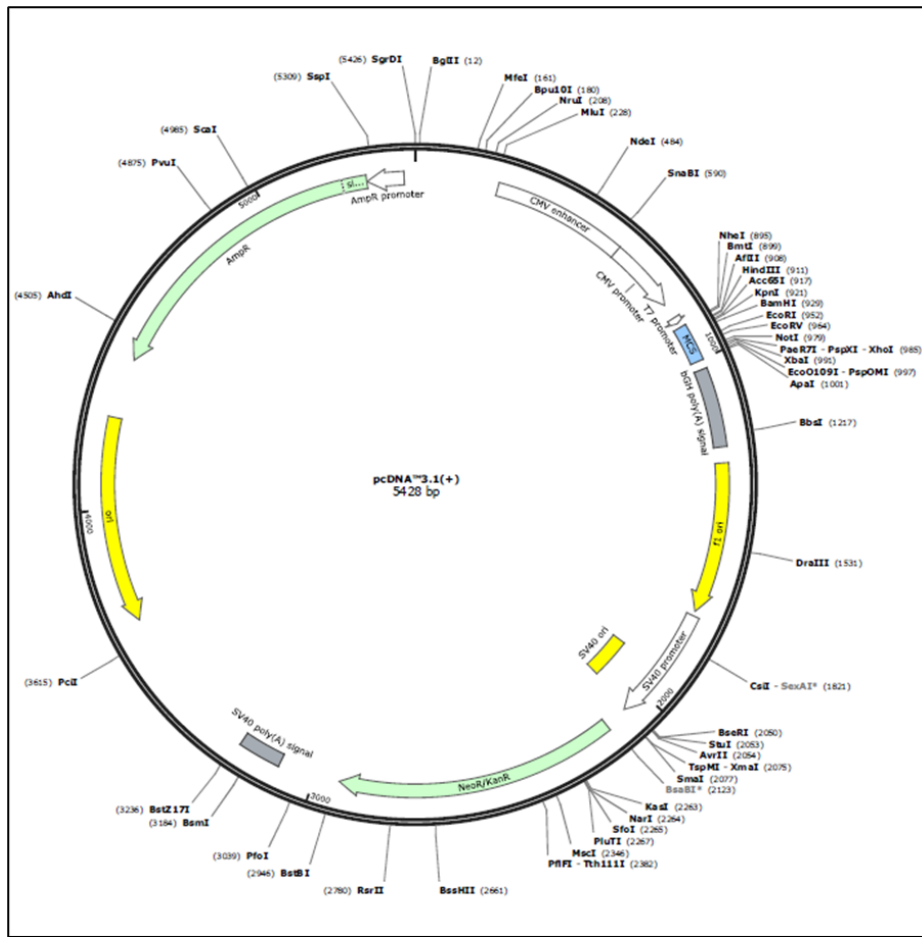


Fig 3.4: pcDNA 3.1 (+) vector

We chose EcoRI and BamHI enzymes for cloning. The 408 bp sequence (from 5' site of FP to 5' site of RP) was analysed in NEB cutter to confirm the absence of EcoRI and BamH1 sites (image attached). These sites were absent and thus these 2 enzymes were finalised.

Forward Primer: MIR149-FP-CP

5' ATCAGGATCCCGCAGAAGGAAGCCAG 3'

Overhangs EcoRI site FP (complementary seq)

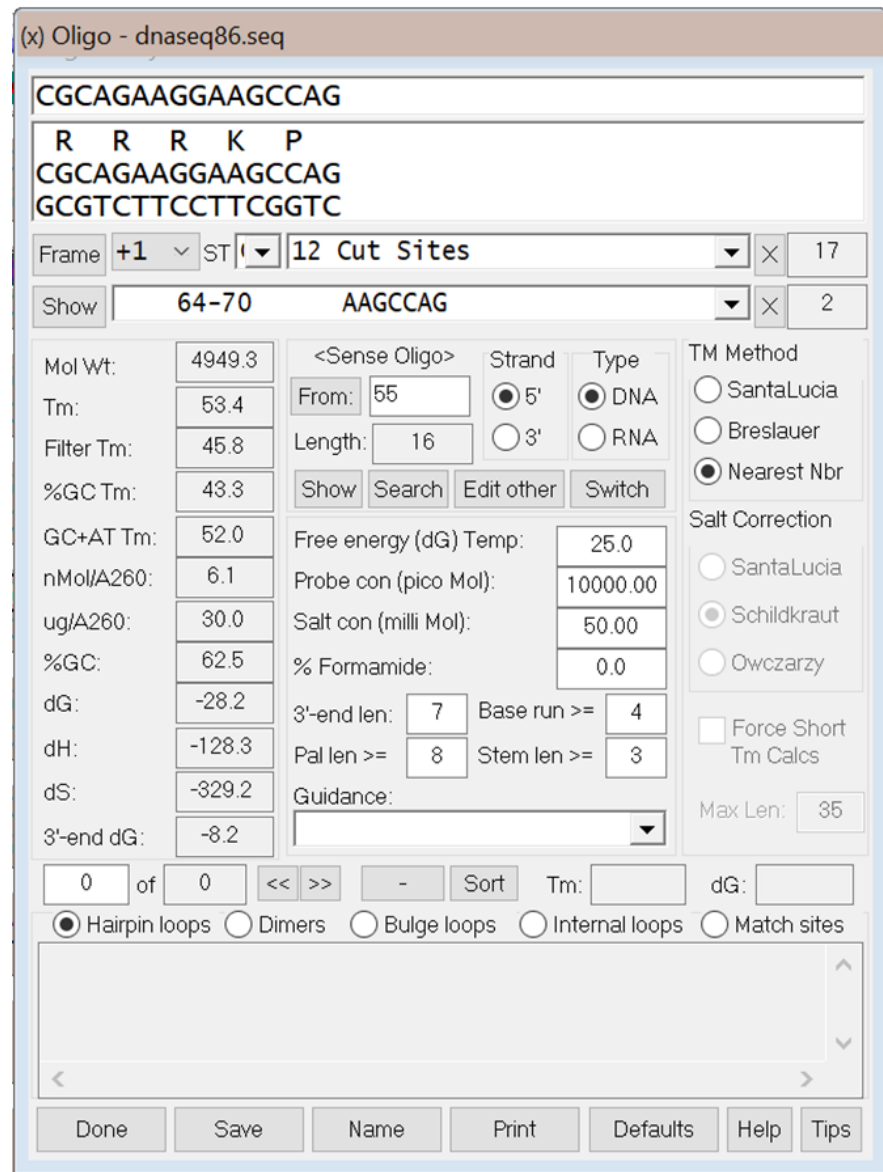


Fig 3.5: Forward primer

Reverse Primer: MIR149-RP-CP

5' ATTA GAATTCT CGTAAGATATGGGAGCTCC 3'

Overhangs EcoRI site RP (complementary seq)

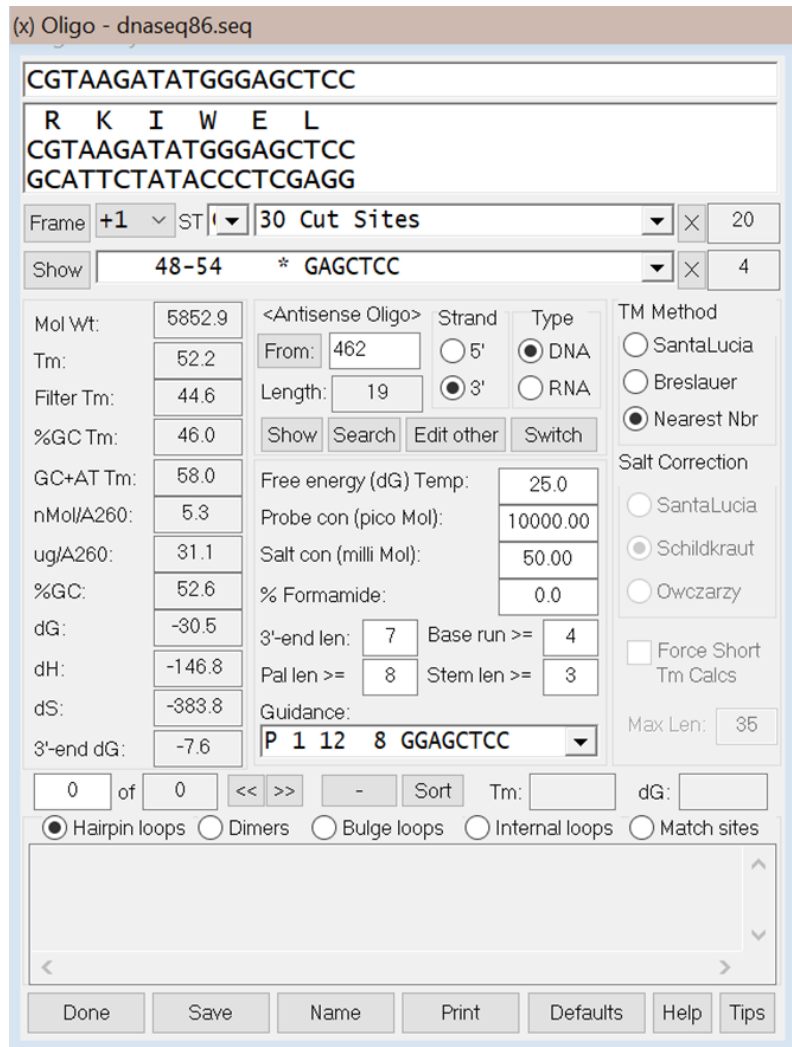


Fig 3.6: Reverse Primer

Overhangs were added which are necessary for polymerase placement. NCBI Primer BLAST was done to identify if the primers are able to clone the desired sequence without off-targets in the genome.

UCSC in silico PCR was run to ensure correct primer design, the results of which are shown in Fig 3.7.

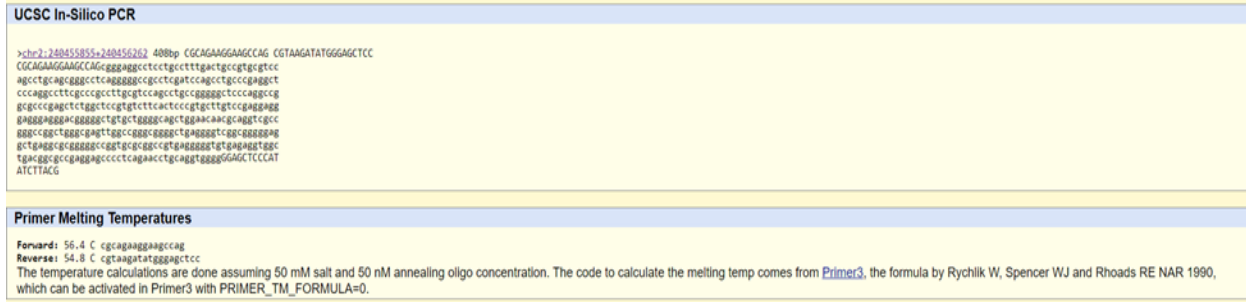


Fig 3.7: Results of UCSC in silico PCR

The final FP and RP sequence and specifications about GC%, Tm and length are noted in Table 4.8

3.3.1.2 Designing Detection Primers

For reverse transcription, a stem loop primer for miR-149 was designed. For detection, a forward primer, designed against the sequence of miR-149-5p and a universal reverse primer were designed and ordered.

3.3.2 Preparation of Overexpression Construct of miR-149

3.3.2.1 Temperature Standardisation of Cloning Primers

The temperature of the primers according to the ThermoFisher Tm Calculator was 59.7°C. We set 20µL of PCR reactions at a 10°C gradient from 54°C to 64°C to account for fluctuations. The PCR reaction mixture comprised 1X buffer, 0.5µM of forward and reverse primers, 100 ng of genomic DNA template from IOMM Lee cells, 0.2 mM of dNTP mix and 0.4 U of Phusion polymerase. Each reaction was made up to 20µL with PCR water.

3.3.2.2 PCR Amplification

miR-149 was amplified according to the reaction composition and temperatures established in 3.3.2.1. The PCR cycling conditions were as follows-

Initial denaturation - 98°C for 1 min 50s

Cyclic denaturation- 98°C for 30s

Cyclic annealing- 62°C for 30s

Cyclic extension- 72°C for 45s.

Final Extension- 72°C for 8 min.

Hold at 4°C.

3.3.2.3 Gel Elution

Due to some non-specific smaller sized products obtained previously, we ran the entire PCR sample obtained above on 2% agarose gel. The band corresponding to our amplified DNA (408 bp) was excised from the agarose gel after visualisation on a UV transilluminator and binding buffer equal to the mass of the excised fragment was added to the MCT. This was then incubated at 56 degrees in a dry bath until the gel dissolved. The entire liquified solution was then passed through the column, followed by subsequent washing and dry spinning steps, to final elution in buffer volume 35 ul. This was then quantified using Nanodrop.

3.3.2.4 Restriction Enzyme Digestion

The pcDNA 3.1+ plasmid and the purified insert/amplicon were digested with EcoRI and BamHI to generate compatible ends. The reaction mixture comprised 500 ng template, 1U EcoRI, 2U BamHI and 2X Tango buffer. Note: Twice the amount of BamH1 was used as per the recommendations obtained using Thermo double digest calculator for 2X Tango Buffer. (Fig x).

Double Digestion with **BamHI**, **EcoRI**

We recommend:

2X Tango buffer
2-fold excess of **BamHI**
EcoRI
Incubate at 37°C

Other options (presented in the order of decreasing restriction enzyme activity):

1. **BamHI** buffer
BamHI
2-fold excess of **EcoRI**
Incubate at 37°C
2. **EcoRI** buffer
2-fold excess of **BamHI**
EcoRI
Incubate at 37°C
3. R buffer
BamHI
EcoRI
Incubate at 37°C

Reaction Conditions for Restriction Enzymes in Thermo Scientific Five Buffer System

	Incubation temp.	Recommended buffer	Units for overnight incubation	Thermal inactivation	Restriction enzyme activity, %					
					B	G	O	R	Tango Buffer	
									1X	2X
BamHI	37°C	BamHI	0.5	80°C(10u)	20-50*	100	20-50	50-100*	100*	50-100
EcoRI	37°C	EcoRI	0.2	65°C	NR(0-20)	NR	100	100*	NR	100

Fig 3.8: Thermo double digest calculator for Tango Buffer

The volume was made up to 50 μ L with nuclease free water. The digestion mixes were run on 1% agarose gel. The bands corresponding to appropriate digested vector and insert sizes were then gel purified as per protocol described above. These digested fragments were then quantified using Nanodrop.

3.3.2.5 Ligation

The cut plasmid and insert were used to prepare ligation mixtures of insert:vector ratios 5:1 and 7:1, calculated using NEBiocalculator. The reaction mixture comprised linear vector, insert, 10X T4 DNA Ligase Buffer and T4 DNA Ligase (5 weiss unit/ μ l). The reaction volume was made up to 20 μ L with nuclease free water. Ligation was performed overnight at 4°C.

3.3.2.6 Transformation

10 ul of the ligation reaction mixture was used to transform competent E. coli DH5 alpha cells which were then plated on a Agar containing Ampicillin as a selection marker. The plate transformed with the 5:1 ratio is henceforth referred to as plate A and the plate with the 7:1 ratio as B.

3.3.2.7 Validation of presence of miR-149 insert in colonies

3.3.2.7.1 Colony PCR

3 among the colonies obtained after O/N incubation of transformed competent cells at 37 degrees were chosen to perform colony PCR. A part of the colonies was mixed in 10ul of nuclease free water and incubated at 95 degrees for 10 minutes (to obtain genetic material in the solution after bacterial cells lysis). 2 ul of this solution was used as template for colony pcr reaction (20 ul per colony using the same PCR protocol). The mixes were then run on 2% agarose gel to visualise and identify positive colonies.

3.3.2.7.2 Plasmid Extraction and Digestion

Colonies showing presence of insert (via colony PCR) were then used to make O/N primary culture (5 ml LB medium with 5 ul Ampicillin, cultured O/N at 37 degrees and 180 rpm). The

turbid primary culture (O/N) was then pelleted down and samples were further processed to extract plasmids using the QIAprep Spin Miniprep Kit. These plasmids were digested with 1U EcoRI, 2U BamHI and 2X Tango buffer to detect the presence of miR-149 insert.

3.3.2.7.3 Sequencing

For final verification, the clones were sent for Sanger Sequencing using the CMV forward primer: 5' CGCAAATGGGCGGTAGGCGTG 3'.

3.3.3 Transfection of miR-149 clone in Iomm Lee cell line

IOMM Lee cells were seeded in a 6 well plate at seeding density 2,00,000 cells/wells. 24 hours post seeding, these cells were transfected with 3 ug of miR-149 clone and pcDNA empty vector (as control) in respective wells. 4ul of Lipofectamine was used per well to generate complexes with respective plasmid. OPTI-MEM reduced serum media was used for complex formation.

3.3.4. RNA extraction

RNA lysates from cells after 48 hours post transfection with miR-149-clone and pcDNA vector, respectively were obtained using 500 ul of RLT buffer (with 5 ul beta mercaptoethanol). These were then processed to obtain total RNA using the Qiagen RNeasy Mini Kit, involving binding, washing, and elution steps. RNA was eluted in 50 ul of nuclease free water and quantified using Nanodrop.

Chapter 4

Results and Discussion

4.1 Bioinformatics Analyses

Previous bioinformatic analysis identified the long noncoding RNA H19 as the most dysregulated lncRNA across all three Meningioma grades w.r.t controls. H19 expression was indicative of a grade dependent increase, with highest dysregulation in advanced grade (grade 3). We wanted to explore H19-regulated coding and noncoding signatures in meningioma. Thus, the 75 patient samples, previously part of the study, were characterised into “high H19” and “low H19” groups on the basis of their normalised expression counts relative to a median count of 201.99.

Figure 4.1 is a visualisation of the number of cases of high and low H19 counts for each parameter, as it allows us to make certain insightful inferences. We notice that an equal number of cases with high and low H19 counts are observed on both sides of our arbitrary age division boundary at 45 years. The samples are approximately evenly divided on the basis of sex with 35 male, and 39 female patients. The males exhibit a greater high to low H19 ratio (20:15) as opposed to (17:22) for females. We notice that the number of cases with high H19 counts are lower in grade 1 Meningiomas, but as the grade increases and the tumours turn malignant, the number of cases with high H19 counts surpasses those with low. This is clearly visible in the plot for grades 2 and 3, where the high H19 count cases go from 54.54% of grade 3 cases to 87.5% of grade 3 cases. The total number of cases per grade drop across grades, but this is explicable by the rarity of higher grade Meningiomas. The proportion of high H19 count cases also increases as we go from non-recurrent (44.4%) to recurrent (61.9%) cases.

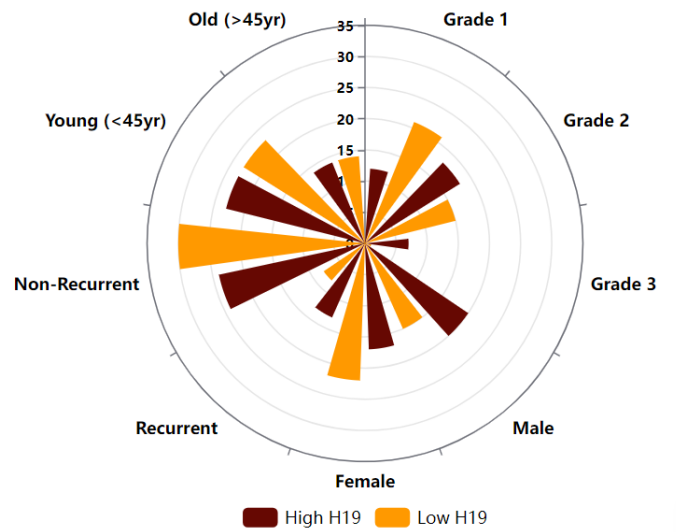


Figure 4.1: Proportion of cases of high and low H19 counts across parameters in the AIIMS dataset

Table 4.1: Analysis of AIIMS dataset classified on the basis of H19 counts

Sr. No.	Characteristic	Classification	Total Cases (n = 75)	High H19 (n = 37)	Low H19 (n = 38)
1	Age	< 60	63 (84%)	31 (49.2%)	32 (50.8%)
		> = 60	12 (16%)	6 (54.54%)	5 (45.45%)
2	Sex	Male	36 (48%)	20 (55.55%)	16 (44.44 %)
		Female	39 (52%)	17 (43.58%)	22 (56.41%)
3	Grade	Grade 1	34 (45.33%)	13 (38.23%)	21 (61.67%)
		Grade 2	35 (46.67%)	18 (51.43%)	17 (48.57%)
		Grade 3	6 (8%)	6 (100%)	0
4	Recurrence	Recurrent	21 (28%)	13 (61.9%)	8 (38.09%)
		Non-Recurrent	54 (72%)	24 (44.44%)	30 (55.55%)
5	Grade+ Recurrence	Grade 1 + Recurrent	11 (14.67%)	4 (36.36%)	7 (63.63%)
		Grade 1 + Non-Recurrent	23 (30.67%)	9 (39.13%)	14 (60.8%)
		Grade 2 + Recurrent	6 (8%)	5 (83.33%)	1 (16.66%)
		Grade 2 + Non-Recurrent	29 (38.67%)	13 (44.83%)	16 (55.17%)
		Grade 3 + Recurrent	4 (5.33%)	4 (100%)	0
		Grade 3 + Non-Recurrent	2 (2.67%)	2 (100%)	0
5	Subtype	Meningothelial (G1)	10 (13.33%)	6 (60%)	4 (40%)
		Transitional (G1)	16 (21.33%)	5 (31.25%)	11 (68.75%)
		Fibrous (G1)	3 (4%)	2 (66.66%)	1 (33.33%)
		Angiomatous (G1)	4 (5.33%)	0	4 (100%)
		Secretory (G1)	1 (1.33%)	0	1 (100%)
		Atypical (G2)	31 (41.33%)	18 (58.06%)	13 (41.93%)
		Clear Cell (G2)	2 (2.66%)	0	2 (100%)
		Chordoid (G2)	2 (2.66%)	0	2 (100%)
		Anaplastic (G3)	6 (8%)	6 (100%)	0
6	MIB LI	Low (< = 6)	39 (52%)	16 (41.02%)	23 (58.97%)
		Moderate (> 6, < 20)	26 (34.66%)	13 (50%)	13 (50%)
		High (>=20)	10 (13.33%)	8 (80%)	2 (20%)

4.1.1 Differentially Expressed Genes

The raw counts of mRNAs previously identified in the study were analysed for differential expression between high and low H19 groups. This analysis was performed in R using the DeSeq2 package¹⁸. The obtained list of dysregulated genes was subjected to cutoffs to ensure significance. Only entries with an adjusted p-value < 0.05 and absolute log 2 fold change > 1 were retained. This implies that the final list of differentially expressed genes (DEGs) only has genes that were increased to over 2x or reduced by over 0.5x in high H19 count samples with respect to low, with over 95% confidence. This is visualised in Fig 4.2.

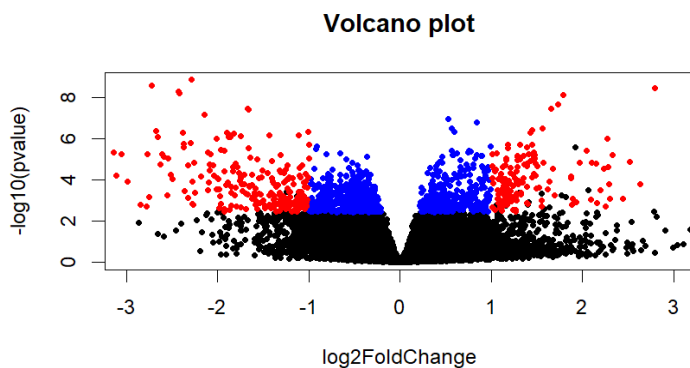


Fig. 4.2: Volcano plot showing significant ($\text{padj} < 0.05$, blue) and significant $+ |\text{log 2 fold change}| > 1$ (red) genes from the differential gene expression analysis result.

A total of 222 genes were found significantly upregulated while 249 were downregulated. The top 20 DEGs are shown in Table 4.2.

Table 4.2: List of top 20 significant differentially expressed genes obtained after analysis in R

S. No.	Upregulate Gene	log2 Fold Change	p adjusted	Downregulate Gene	log2 Fold Change	p adjusted
1	AGTR2	3.18	0.026483	FUT9	-3.92	0.000015
2	POTEM	2.91	0.027514	ELMOD1	-3.36	0.000046
3	OR4M2	2.81	0.006171	CHL1	-3.14	0.001337
4	GPC3	2.80	0.000015	CDH18	-3.12	0.004992
5	MYF6	2.78	0.003636	SSTR1	-3.05	0.001343
6	KRT14	2.64	0.008287	RIMS2	-2.99	0.007226
7	PPP1R3A	2.54	0.011185	FRG2B	-2.86	0.012688
8	SLITRK6	2.52	0.002190	C11orf87	-2.85	0.032186
9	MYH2	2.44	0.021801	CLVS2	-2.78	0.035738
10	TDRD12	2.33	0.001391	ADCYAP1R1	-2.77	0.001343
11	IGF2BP1	2.30	0.020706	SLCO1A2	-2.75	0.019173
12	DMBT1	2.29	0.008236	NEGR1	-2.72	0.000015
13	TNNI1	2.28	0.002872	GPM6A	-2.67	0.000338
14	MYBPC2	2.27	0.000469	MCHR2	-2.66	0.041833
15	KRTAP10-2	2.26	0.038744	TRHDE	-2.65	0.000422
16	XIRP2	2.26	0.035504	FAM181B	-2.62	0.002470
17	SOX11	2.24	0.003067	AKR1B10	-2.61	0.001343
18	NMU	2.20	0.012548	APOD	-2.59	0.001507
19	MYH1	2.16	0.027707	PCDH11X	-2.55	0.017982
20	MMP1	2.16	0.003894	CNTNAP2	-2.55	0.001690

4.1.2 Comparison with Literature

Among the 306 genes found to be upregulated in grade 3 Meningioma with respect to grade 1 Meningioma in at least 2 GEO datasets, 58 were common with the 222 upregulated genes in our data (high vs low H19 groups) (Fig 4.3, List 1). Similarly, of the 28 genes found dysregulated in recurrent with respect to non-recurrent meningioma in at least 2 GEO datasets, 16 were common with our upregulated genes (Fig 4.3, List 2). Interestingly 15 genes among these were common to both lists: SOX11, ASPM, CENPF, KIAA0101, TRIP13, BUB1B, NUSAP1, DTL, UBE2C, BUB1, NCAPG, PBK, KIF11, AURKA, CCNB2. These 15 genes are thus associated with higher grade and recurrent meningiomas and are also potentially regulated by H19. Grade 3 Meningioma with respect to grade 1 Meningioma showed 248 genes downregulated that were common to at least 2 GEO datasets. Of these, only 8 were common with the 249 downregulated genes in patient samples with high vs low H19 lncRNA counts (Fig 4.3, List 3). Only 1 gene- GPX3, was found downregulated in both - high vs low groups and the 29 recurrent vs non-recurrent meningioma comparisons from at least 2 GEO databases. GPX3 was also present in List 3. This implies that GPX3 is associated with lower grade and non-recurrent meningiomas and is also potentially regulated by H19.

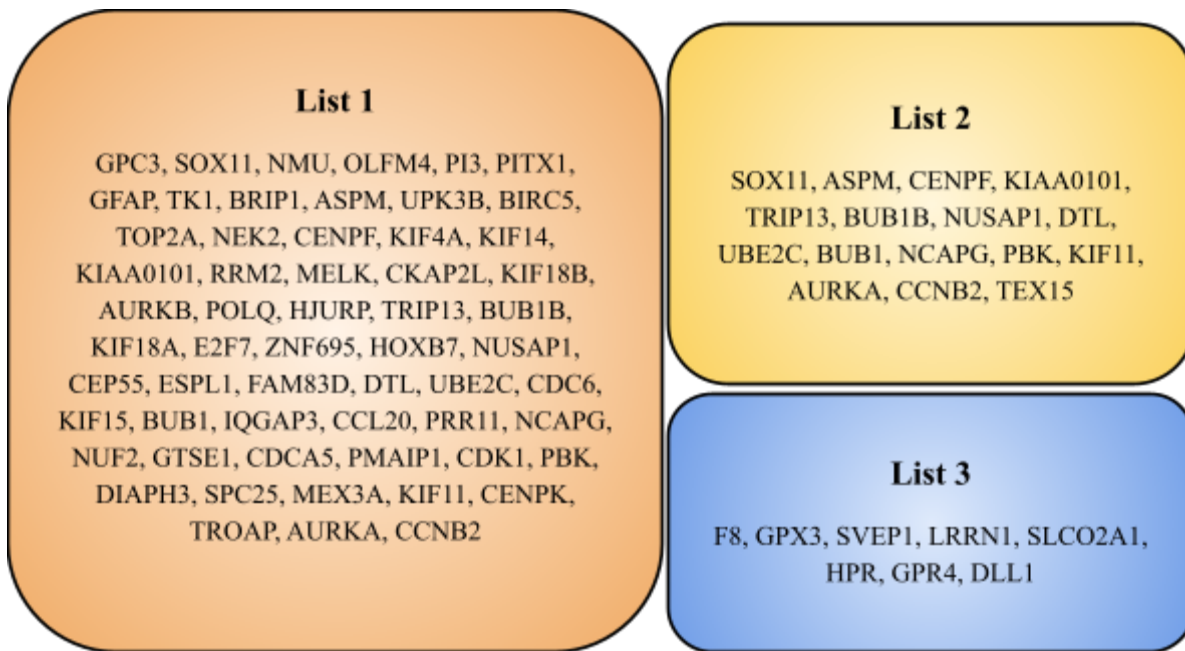


Figure 4.3 Comparison of differentially expressed genes with GEO datasets List 1: Upregulated DEGs common with genes upregulated in grade 3 Meningioma with respect to grade 1 Meningioma in at least 2 GEO datasets, List 2: Upregulated DEGs common with genes upregulated in recurrent meningioma with respect to non-recurrent meningioma in at least 2 GEO datasets, List 3: Downregulated DEGs common with genes downregulated in grade 3 Meningioma with respect to grade 1 Meningioma in at least 2 GEO datasets

4.1.3 Gene Ontology Analysis

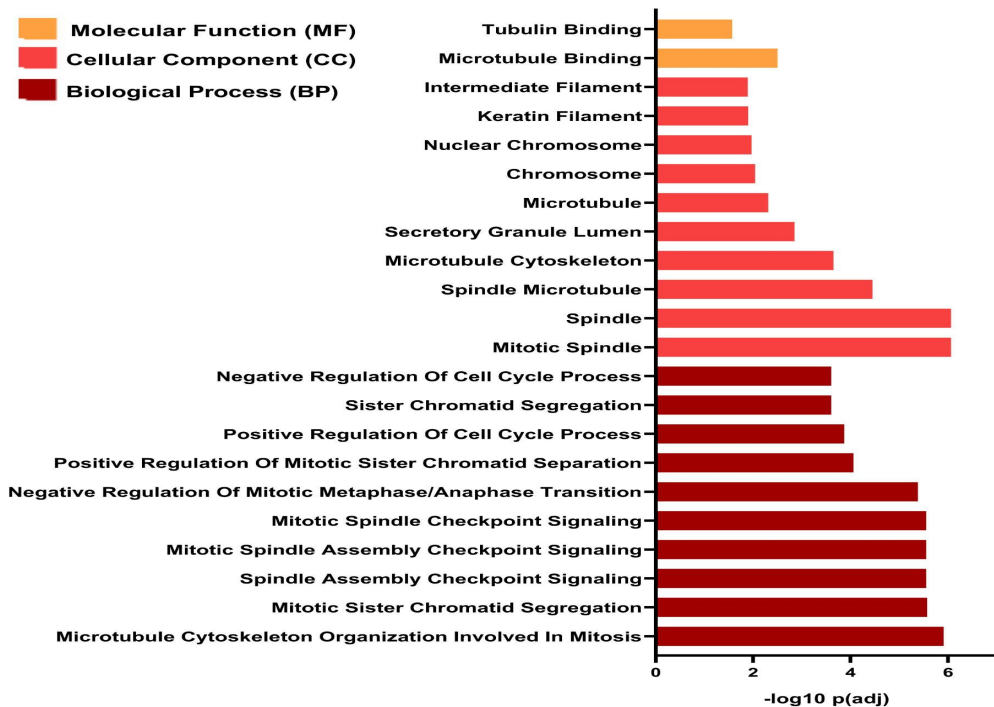


Fig 4.4 Gene Ontology analysis for Upregulated genes

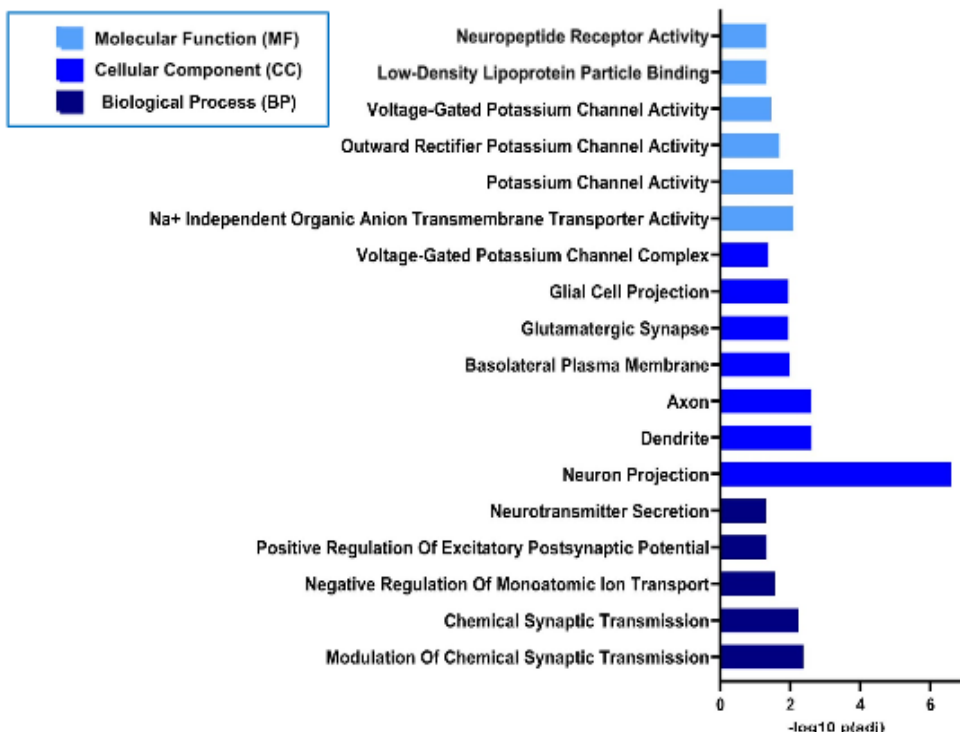


Fig 4.5 Gene Ontology analysis for Downregulated genes

4.1.3.1 Biological Processes

A total of 101 biological processes were significantly enriched in association with the upregulated DEGs. Supplementary Table S1 shows the top 20 of these. The majority of these were related to mitosis. The downregulated genes were associated with 5 significantly enriched pathways, mostly pertaining to synaptic transmission. These are shown in Supplementary Table S2.

4.1.3.2 Molecular Function

The products of the upregulated DEGs were implicated in 2 molecular functions: microtubule binding and tubulin binding, while those of the downregulated DEGs were implicated in 6: Sodium-Independent Organic Anion Transmembrane Transporter Activity, Potassium Channel Activity, Outward Rectifier Potassium Channel Activity, Voltage-Gated Potassium Channel Activity, Low-Density Lipoprotein Particle Binding, Neuropeptide Receptor Activity. All these molecular functions are tabulated in Supplementary Table S3 and S4.

4.1.3.3 Cellular Components

28 Cellular components were found overrepresented in association with the upregulated genes, while this number was 7 for downregulated genes. These are shown in Supplementary Table S5 and S6.

4.1.4 Pathway Analysis

The upregulated DEGs are significantly implicated in 3 pathways: Cell cycle, p53 signalling and *S. aureus* infection, while the downregulated DEGs are associated with 2 pathways: Neuroactive ligand-receptor interaction and cAMP signalling pathway. This information is tabulated in Supplementary Table S7 and S8.

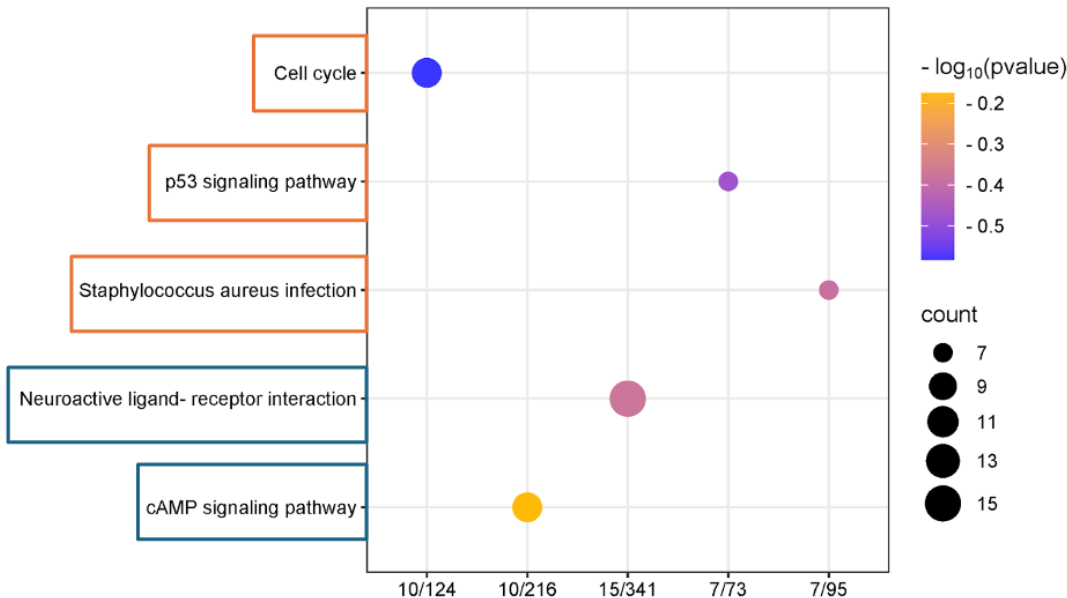


Fig 4.6: Pathways in which the upregulated DEGs are significantly implicated.

4.1.5 Identification of Oncogenes and Tumour Suppressor Genes followed by overlap with meningioma grade 3 associated gene signature

To identify established onco and tumour suppressor genes in our data, we intersected our list with the list obtained from oncoKB. Interestingly, we found 9 oncogenes (HOXA11, BRIP1, CD70, TOP2A, DUSP2, POLQ, BLM, TRIP13, ESCO2, SLC1A2, FGF1, EPHA5, FGF12) that were upregulated in our data set and 9 tumour suppressor genes(GPC3, MKI67, CENPA, AURKB, BUB1B, NUF2, CDKN2A, PMAIP1, AURKA, CAMTA1, PRDM16, KDR, MDC1) that were downregulated in our data. We further intersected the list of differentially expressed genes between grade 3 and control samples, identified previously, with our list of DEGs between high and low H19 groups. We identified 16 DEGs to be common between the two (GPC3, HOXA11, BRIP1, CD70, TOP2A, DUSP2, MKI67, CENPA, AURKB, POLQ, BLM , TRIP13, BUB1B, ESCO2, NUF2, CDKN2A, GTSE1, PMAIP1, AURKA, CAMTA1, PRDM16, KDR, MDC1, FOLH1, SLC1A2, FGF1, EPHA5 and FGF12) which showed similar expression trends (up/downregulation). The intersection and subsequent analysis with the oncoKB data revealed 4 oncogenes common to the DEGs on the basis of H19 counts and Meningioma grades, which were upregulated in meningioma patient samples, in accordance with the expected trend. The analysis also uncovered 2 downregulated DEGs common to both lists to be tumour suppressor

genes. Interestingly, 10 genes were found to violate the expectation of finding oncogenes upregulated and TSGs downregulated. SLC1A2, FGF1, EPHA5, FGF12 were the four oncogenes found downregulated while GPC3, MKI67, BUB1B, NUF2, PMAIP1, AURKA are six TSGs that were found upregulated. This may be due to different roles of these genes across cancers, as the oncoKB database covers many different types of cancer and is not specific to Meningioma.

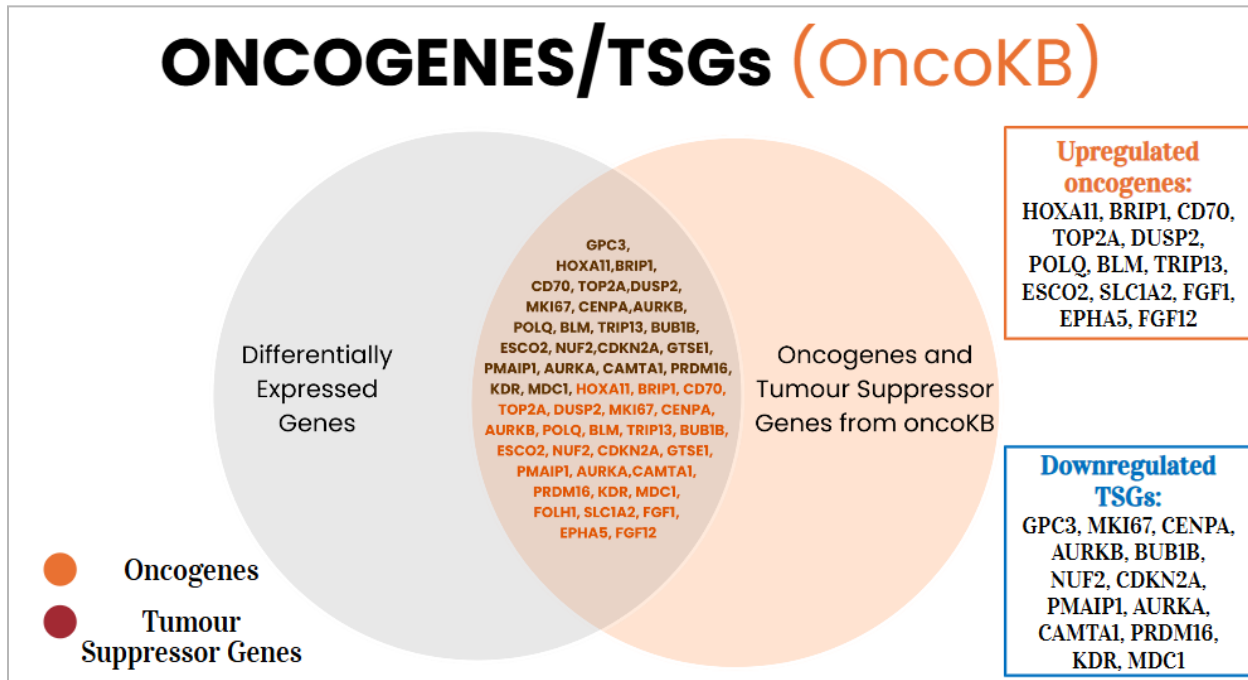


Fig 4.6: Common Oncogenes and Tumour Suppressor genes amongst our Differentially Expressed genes and known cancer related genes from oncoKB

4.1.6 Immune Infiltration Analysis

4.1.6.1 TIMER

On analysing TIMER 2.0 results for significance, we obtain 3 types of immune cells which exhibit significant differences in expression in the samples with low vs high H19 counts - Monocytes, T cell CD8+ and Neutrophils, as shown in Fig. x. Monocytes were found significant by the CIBERSORT algorithm which is effective in deconvoluting detailed subsets of T-cell signatures and provides insights into specific immune responses. T cell CD8+ was detected by

the EPIC algorithm which directly generates scores that can be interpreted as cell fractions, offering a straightforward assessment of immune cell composition. Neutrophils were detected by the MCP-counter method which focuses on quantifying the abundance of immune and stromal cells in tumour samples.

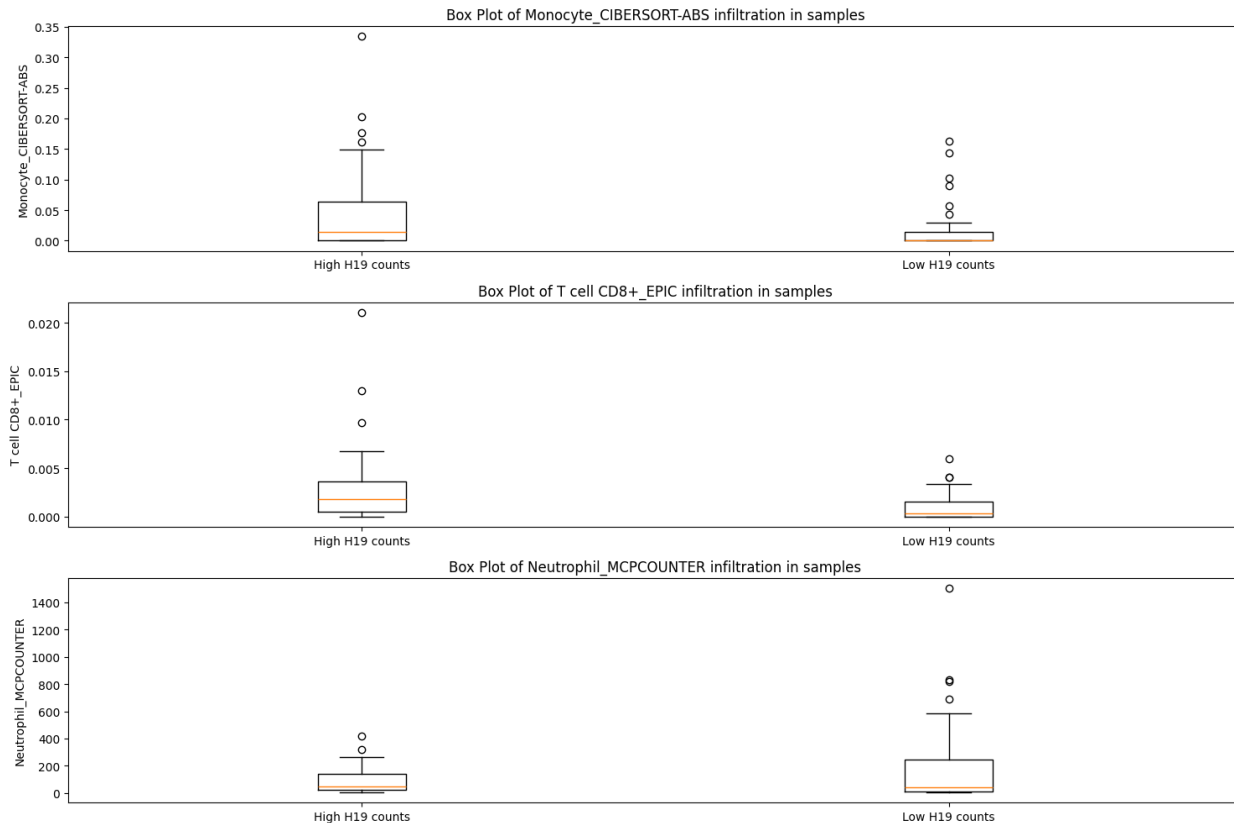


Fig 4.8: Significantly different immune cell infiltration in samples based on H19 count

4.1.6.2 ImmReg

A comparison of the relevant TFs and RBPs obtained from ImmReg with the DEGs, 48 transcription factors and 25 RBPs were found common. The top 5 immune associated roles of these DEGs were Antigen Processing and Presentation, Cytokines, Cytokine Receptors, Antimicrobials and TCR signalling Pathway. These are tabulated in Table 4.3.

Table 4.3: Transcription Factors and Ribosome Binding Proteins common to both DEGs and ImmReg data

TFs common with ImmReg	RBPs common with ImmReg
CENPF	TOP2A
CENPA	MKI67
TRIP13	NUSAP1
MYF6	TDRD12
SOX11	IGF2BP1
HOXA11	UNC45B
ANKRD1	KIF14
HOXB5	POLQ
PITX1	BLM
FOXD3	MYL4
NKX2-5	IGF2BP3
BRIP1	CDKN2A
MYBL2	MEX3A
CSRP3	CELF4
MYOG	KIAA1324
E2F8	CNN1
BLM	NOVA2
E2F7	ADAD2
ZNF695	NOVA1

HOXC4	SYNPO
HOXB7	SNCG
ESPL1	MAP2K6
CDC6	LDB3
BOLA2B	STXBP1
CDKN2A	NDRG2
CEBPE	
CENPK	
ATN1	
CAMTA1	
RAPGEF4	
SATB2	
NFIC	
PRDM16	
ZNF365	
GREB1	
RGS6	
FHL5	
TFCP2L1	
HES5	
SOX5	
SOX8	

PTGER3	
CUX2	
PEG3	
BHLHE22	
ONECUT1	
MYOCD	
BEX1	

4.1.7 Coexpression Analysis

23 of our 471 DEGs were predicted to have positive expression correlation with H19 as obtained from cBioPortal data. These are listed in Table 4.4.

Table 4.4: DEGs predicted to be coexpressed with the H19 long non-coding RNA

Top 20 common genes	Spearman Coefficient	Log 2 Fold Change	Cytoband	p-Value
TNNT3	0.70	1.97	11p15.5	3.20E-19
PHYHIP	0.39	-2.04	8p21.3	9.81E-06
SAA1	0.39	1.82	11p15.1	1.18E-05
KRT14	0.38	2.64	17q21.2	1.38E-05
HOXB5	0.38	2.04	17q21.32	1.64E-05
FOXD3	0.38	1.81	1p31.3	2.06E-05
ACSBG1	0.38	-1.38	15q25.1	2.21E-05
CCL20	0.37	1.14	2q36.3	2.26E-05
ANKRD1	0.37	2.04	10q23.31	2.29E-05
PI3	0.36	2.10	20q13.12	5.85E-05
HOXA11	0.35	2.09	7p15.2	8.61E-05
KRT17	0.35	1.71	17q21.2	9.38E-05
CP	0.34	-1.62	3q24-q25.1	0.00011
TFCP2L1	0.34	-1.28	2q14.2	0.000116
STC1	0.34	-1.41	8p21.2	0.000133
MUC4	0.34	-1.85	3q29	0.000133
APLN	0.33	1.53	Xq26.1	0.0002
ELANE	0.32	1.93	19p13.3	0.000392
GRIK3	0.31	-1.74	1p34.3	0.000558

4.1.8 Protein-Protein Interaction Network construction and identification of Hub Genes

To identify the hub genes among the DEGs regulated by H19, we constructed protein-protein interaction networks using the STRING app (confidence score= 0.700; high confidence) for up and downregulated genes separately. A dense network (205 nodes and 1047 edges; Figure 4.9) was obtained for upregulated genes. To find top modules we used the MCODE plugin in Cytoscape and obtained the topmost cluster (Figure 4.10) consisting of 34 nodes and 516 edges, with score 31.273. The CytoHubba plugin was used to identify top 20 upregulated hub genes (Figure 4.11) using the MCC method (Strongest among 11 methods). These have been tabulated in Table 4.5.

A relatively less connected network (244 nodes and 237 edges; Figure 4.12) was obtained for downregulated genes. To find top modules we used the MCODE plugin in Cytoscape and obtained the topmost cluster (Figure 4.13) consisting of 5 nodes and 10 edges, with score 5. The CytoHubba plugin was used to identify top 20 downregulated hub genes (Figure 4.14) using the MCC method. These have been tabulated in Table 4.6.

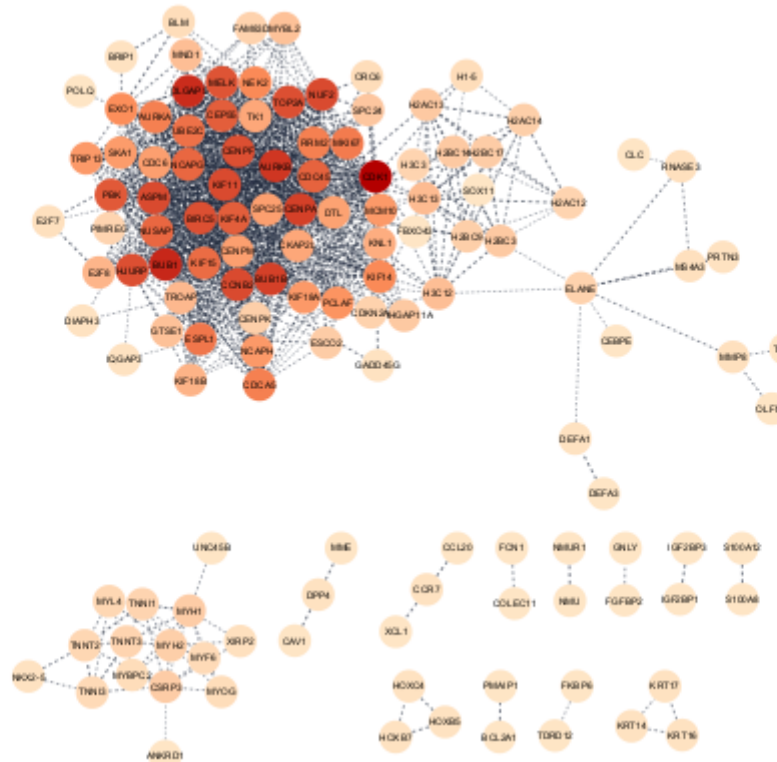


Figure 4.9: Complete network obtained from PPI of upregulated genes

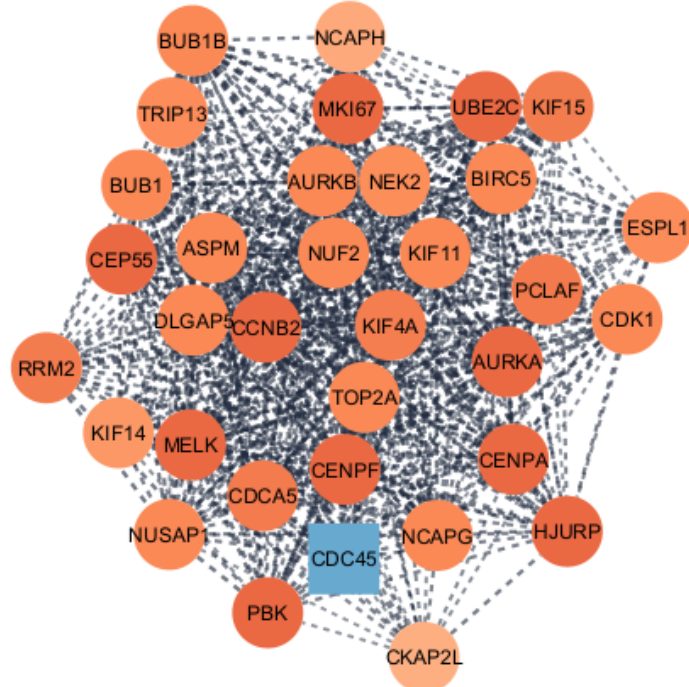


Figure 4.10: First cluster obtained from PPI of upregulated genes

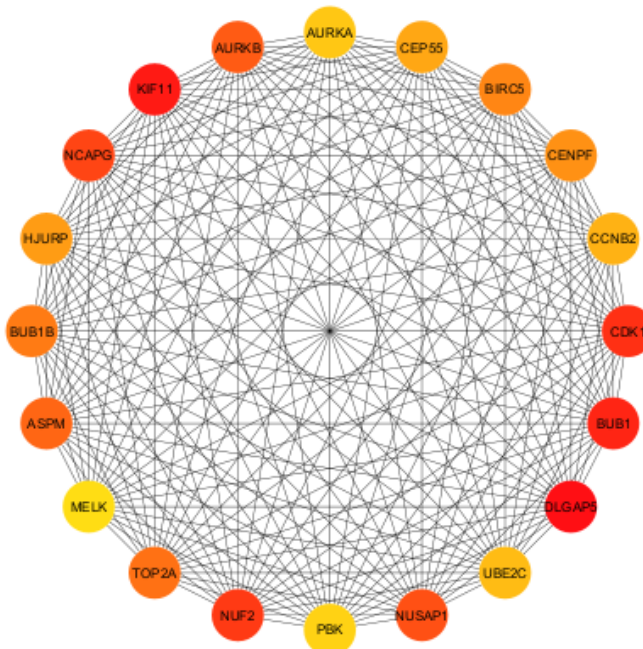


Figure 4.11: Top 20 hub genes from upregulated genes

Table 4.5: Top 20 hub genes from upregulated genes

Hub Gene	Log 2 Fold Change
DLGAP5	1.16
KIF11	1.06
BUB1	1.16
CDK1	1.10
NUF2	1.12
NCAPG	1.13
NUSAP1	1.22
AURKB	1.33
ASPM	1.66
TOP2A	1.48
BUB1B	1.29
BIRC5	1.57
CENPF	1.45
HJURP	1.30
CEP55	1.21
CCNB2	1.01
UBE2C	1.19
AURKA	1.02
PBK	1.10
MELK	1.39

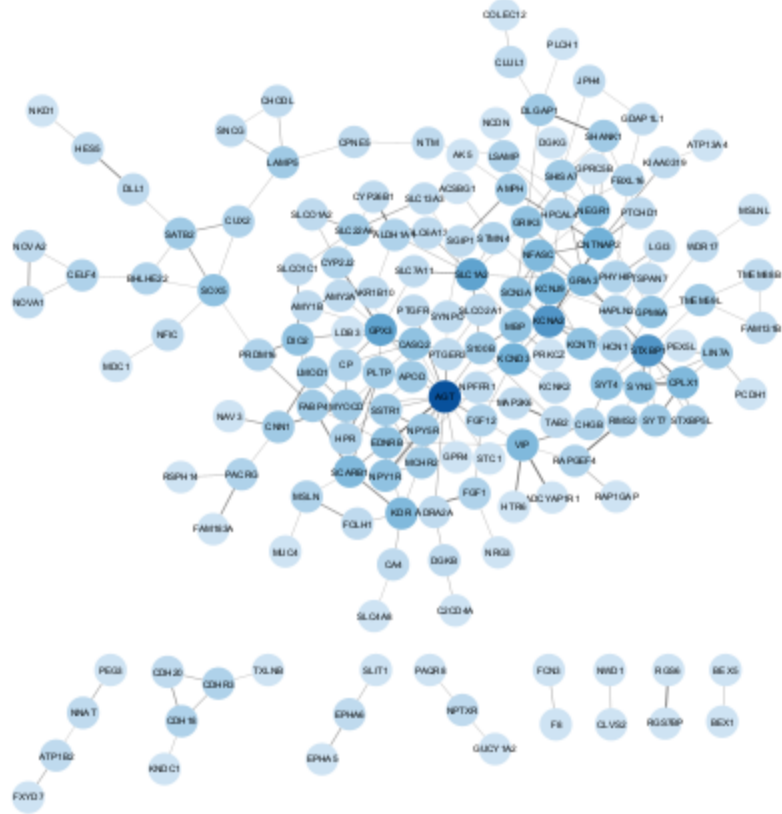


Figure 4.12: Complete network obtained from PPI of upregulated genes

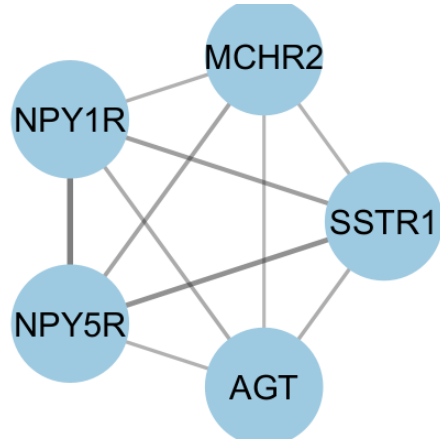


Figure 4.13: First cluster obtained from PPI of downregulated genes

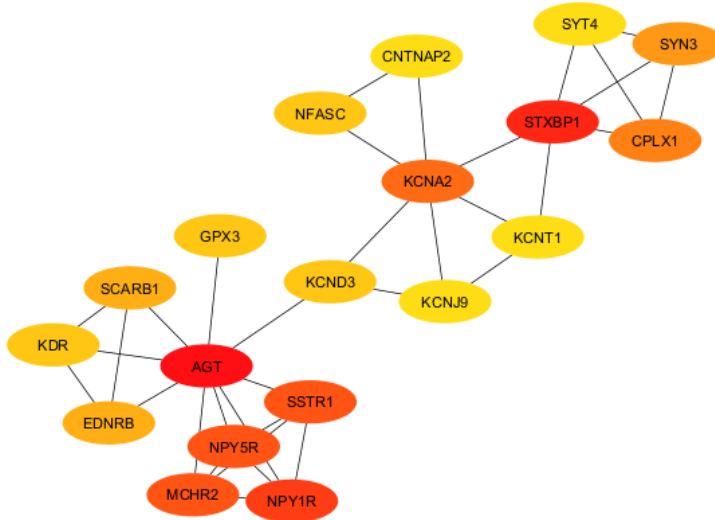


Figure 4.14: Top 20 hub genes from downregulated genes

Table 4.6: Top 20 hub genes from downregulated genes

Hub Gene	Log 2 Fold Change
AGT	-1.90
STXBP1	-1.07
NPY1R	-1.74
NPY5R	-2.25
MCHR2	-2.66
SSTR1	-3.05
KCNA2	-1.26
CPLX1	-1.21
SYN3	-1.58
SCARB1	-1.66
EDNRB	-1.21
SLC1A2	-2.00

NFASC	-1.26
KCND3	-1.12
GPX3	-1.34
KDR	-1.11
KCNJ9	-1.32
SYT4	-1.52
CNTNAP2	-2.55
KCNT1	-2.11

4.1.9 H19 Associated ceRNA Networks

Mirnet 2.0 tool was used to identify the miRNAs that target the upregulated genes in high vs low H19 groups. Among the identified miRNAs, we looked for those known to interact with H19. These H19 interacting miRNAs were overlapped with dysregulated miRNAs in grade 3 meningioma (vs control) from our previous differential miRNA data from the 75 patient samples. Only 5 miRNAs were common to both sets. These miRNAs and their implications in cancers in existing literature are noted in Table 4.7. Among these, 3 miRNAs were upregulated (hsa-miR-20a-5p, hsa-miR-20b-5p and hsa-miR-301a-3p) while 2 were downregulated (hsa-miR-149-5p and hsa-miR-4739) in grade 3 meningioma. We used the above data to construct an lncRNA-miRNA-mRNA interaction network (Figure 4.15)

In accordance with the ceRNA hypothesis H19 might interact with downregulated miRNAs (hsa-miR-149-5p and hsa-miR-4739) which might result in the upregulation of the target mRNAs of these miRNAs. We chose hsa-miR-149-5p as the candidate miRNA to evaluate its interaction with H19 as it is commonly dysregulated in a variety of cancers and its role has not been studied in meningioma. Interestingly, among the predicted targets of hsa-miR-149-5p, 14 genes (BIRC5, PITX1, RRM2, AURKA, HIST1H2AI, ESPL1, AURKA, BIRC5, CENPF, ESPL1, HIST1H2AI, PITX1, RRM2, TOP2A) were also among the top 20 upregulated hub genes in our data and thus might serve as attractive targets.

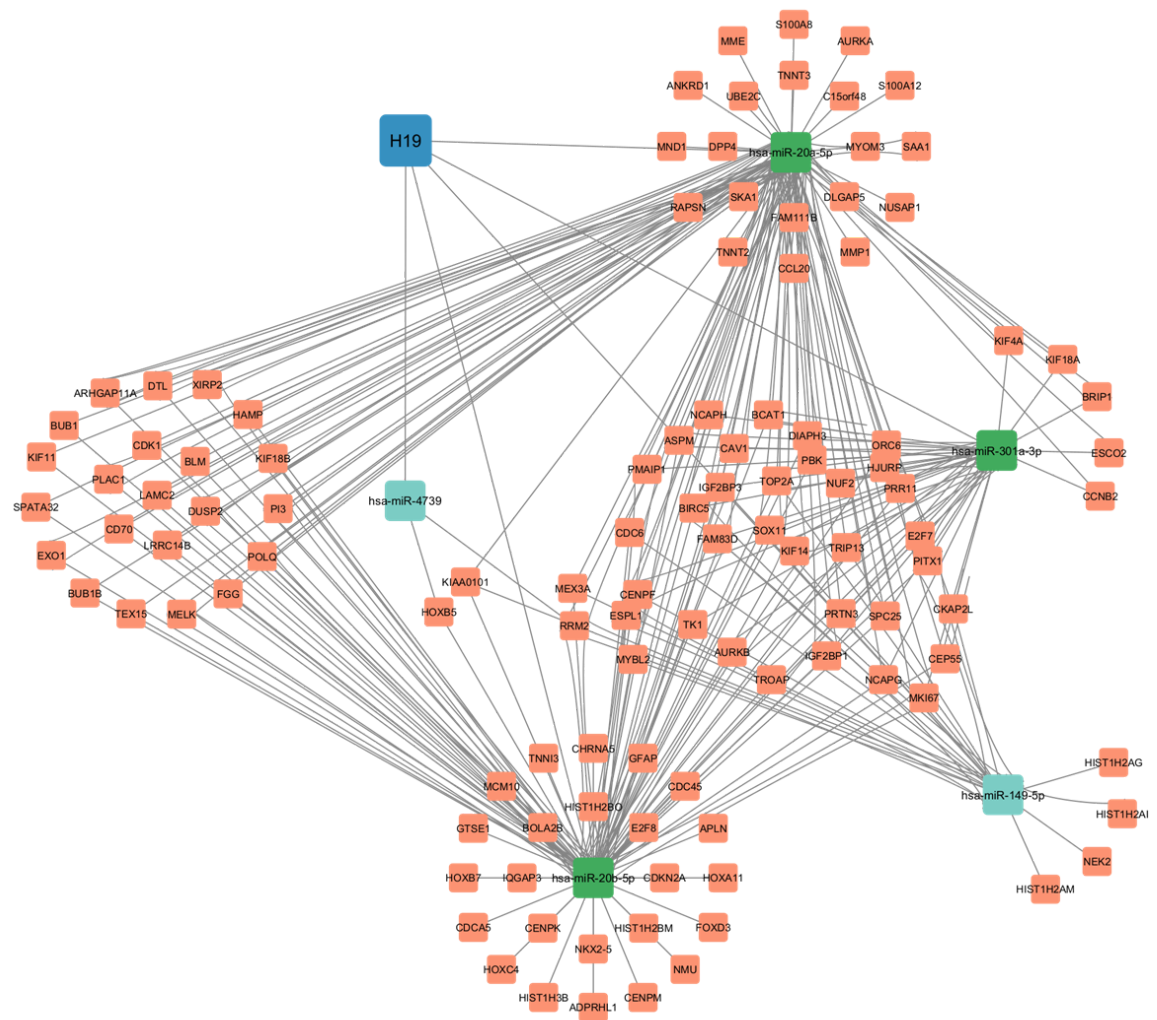


Figure 4.15 lncRNA-miRNA-mRNA interaction network

miRNA	Dysregulation	Implication in cancer studies
hsa-miR-20a-5p	Upregulated	Biomarker for cancer diagnosis and prognosis and therapeutic target in breast cancer, liver cancer, leukaemia etc. ²³
hsa-miR-20b-5p	Upregulated	Overexpressed in cancerous tissues, associated with lymph node metastasis, clinical stage, and overall survival, can promote malignancy of breast cancer cells and hepatocellular carcinoma cell proliferation, migration, and invasion ²⁴
hsa-miR-301a-3p	Upregulated	Promotes triple-negative breast cancer progression ²⁵ , inhibits killing effect of natural killer cell immunotherapy on non-small cell lung cancer cells ²⁶
hsa-miR-149-5p	Downregulated	Regulates inflammatory response, adipogenesis and cell proliferation, can function as an oncogene or tumour suppressor in different cancers ²⁷
hsa-mir-4739	Downregulated	Suppresses tumorigenesis and metastasis of hepatocellular carcinoma ²⁸ , suppresses the tumorigenesis and progression of prostate cancer ²⁹

Table 4.7: miRNAs found common to H19+DEG interactors and AIIMS dysregulated miRNA lists

4.1.10 Candidate miRNA Selection

The candidate miRNA selected for artificially engineered dysregulation and cell based assays to study effects of this regulation was: **hsa-mir-149-5p**. The three upregulated miRNAs have been very thoroughly studied in cancers, leaving little scope for novelty feasible within the time and resource constraints of a B. Tech project. Moreover, experimental validation of the role of upregulated miRNAs in cancer would require cell-based assays post-downregulation, which would require the purchase of antimiR, which is currently financially infeasible. Of the two downregulated miRNAs, hsa-mir-4739 has been implicated in only a few cancers. Meanwhile there is an entire review article detailing the role of hsa-mir-149-5p across cancers²⁷. It details the role of hsa-mir-149-5p in human cancers of the reproductive- breast, ovarian, cervical, prostate; digestive- gastric, hepatocellular, colorectal, oral, esophageal, pancreas; respiratory- lung,

nasopharyngeal; urinary- renal, bladder; endocrine- thyroid; circulatory- leukaemia; nervous-glioma and motor system- osteosarcoma. However, despite being implicated in brain glioblastoma, there are no studies on the role of hsa-mir-149-5p in Meningioma. This makes hsa-mir-149-5p a novel, yet promising, candidate for analysis in Meningioma.

To test interaction of H19 and miR-149, the target sequence of miR-149-5p in H19 was confirmed from StarBase as shown in Fig 4.16.

miRNA	GeneID	GeneName	GeneType	TargetSite	Alignment	Type	TDMDScore	AgoExpNum	CleaveExpNum	phyloP	Pan-Cancer
hsa-149-5p	ENSG00000130600	H19	lncRNA	chr11:1997543-1997563[.]	Target: 5' UGGAGAGAG-3' : mRNA : 3' CCACACAUUCUUGCCUCCU 5'	7mer-m8	1.2758	1	0	-0.063	0

Description:
Here, we presented the miRNA-target interactions by intersecting the predicting target sites of miRNAs with binding sites of Ago protein, which were derived from CLIP-seq data. We also introduced a new algorithm called **TDMDScore** to systematically scan the miRNA-target interactions and evaluated the potential interactions that triggered **target-directed microRNA degradation (TDMD)**. A higher TDMDScore indicates that the miRNA-target is more likely to trigger the TDMD. The interactions of miRNA-IncRNA were predicted by using miRanda program.

Fig 4.16: Target sequence of miR-149-5p in H19 from StarBase

Ensembl transcript comparison was used to establish which transcripts of H19 contained the target sequence as shown in Fig 4.17.

H19	6961	AGCTGGGACGATGGGCTGAGCTAGGGC	TGGAAAAGAAGGGGGAGCCAGG	CATTCA	TCCC	GGT	CAC	TTTG	GGTA	CAGGGGAGCTGGTGGGCAGGGT	7080	
H19-201	6961	AGCTGGGACGATGGGCTGAGCTAGGGC	TGGAAAAGAAGGGGGAGCCAGG	CATTCA	TCCC	GGT	CAC	TTTG	GGTA	CAGGGGAGCTGGTGGGCAGGGT	7080	
H19-202	6961	AGCTGGGACGATGGGCTGAGCTAGGGC	TGGAAAAGAAGGGGGAGCCAGG	CATTCA	TCCC	GGT	CAC	TTTG	GGTA	CAGGGGAGCTGGTGGGCAGGGT	7080	
H19-203	6961	AGCTGGGACGATGGGCTGAGCTAGGGC	TGGAAAAGAAGGGGGAGCCAGG	CATTCA	TCCC	GGT	CAC	TTTG	GGTA	CAGGGGAGCTGGTGGGCAGGGT	7080	
H19-204	6961	AGCTGGGACGATGGGCTGAGCTAGGGC	TGGAAAAGAAGGGGGAGCCAGG	CATTCA	TCCC	GGT	CAC	TTTG	GGTA	CAGGGGAGCTGGTGGGCAGGGT	7080	
H19-205	6961	AGCTGGGACGATGGGCTGAGCTAGGGC	TGGAAAAGAAGGGGGAGCCAGG	CATTCA	TCCC	GGT	CAC	TTTG	GGTA	CAGGGGAGCTGGTGGGCAGGGT	7080	
H19-206	6961	AGCTGGGACGATGGGCTGAGCTAGGGC	TGGAAAAGAAGGGGGAGCCAGG	CATTCA	TCCC	GGT	CAC	TTTG	GGTA	CAGGGGAGCTGGTGGGCAGGGT	7080	
H19-207	6961	AGCTGGGACGATGGGCTGAGCTAGGGC	TGGAAAAGAAGGGGGAGCCAGG	CATTCA	TCCC	GGT	CAC	TTTG	GGTA	CAGGGGAGCTGGTGGGCAGGGT	7080	
H19-208	6961	AGCTGGGACGATGGGCTGAGCTAGGGC	TGGAAAAGAAGGGGGAGCCAGG	CATTCA	TCCC	GGT	CAC	TTTG	GGTA	CAGGGGAGCTGGTGGGCAGGGT	7080	
H19-209	6961	AGCTGGGACGATGGGCTGAGCTAGGGC	TGGAAAAGAAGGGGGAGCCAGG	CATTCA	TCCC	GGT	CAC	TTTG	GGTA	CAGGGGAGCTGGTGGGCAGGGT	7080	
H19-210	6961	AGCTGGGACGATGGGCTGAGCTAGGGC	TGGAAAAGAAGGGGGAGCCAGG	CATTCA	TCCC	GGT	CAC	TTTG	GGTA	CAGGGGAGCTGGTGGGCAGGGT	7080	
H19-211	6961										-----	7080
H19-212	6961	AGCTGGGACGATGGGCTGAGCTAGGGC	TGGAAAAGAAGGGGGAGCCAGG	CATTCA	TCCC	GGT	CAC	TTTG	GGTA	CAGGGGAGCTGGTGGGCAGGGT	7080	
H19-213	6961	AGCTGGGACGATGGGCTGAGCTAGGGC	TGGAAAAGAAGGGGGAGCCAGG	CATTCA	TCCC	GGT	CAC	TTTG	GGTA	CAGGGGAGCTGGTGGGCAGGGT	7080	
H19-214	6961	AGCTGGGACGATGGGCTGAGCTAGGGC	TGGAAAAGAAGGGGGAGCCAGG	CATTCA	TCCC	GGT	CAC	TTTG	GGTA	CAGGGGAGCTGGTGGGCAGGGT	7080	
H19-215	6961	AGCTGGGACGATGGGCTGAGCTAGGGC	TGGAAAAGAAGGGGGAGCCAGG	CATTCA	TCCC	GGT	CAC	TTTG	GGTA	CAGGGGAGCTGGTGGGCAGGGT	7080	
H19-216	6961	AGCTGGGACGATGGGCTGAGCTAGGGC	TGGAAAAGAAGGGGGAGCCAGG	CATTCA	TCCC	GGT	CAC	TTTG	GGTA	CAGGGGAGCTGGTGGGCAGGGT	7080	
H19-217	6961										-----	7080
H19-218	6961	AGCTGGGACGATGGGCTGAGCTAGGGC	TGGAAAAGAAGGGGGAGCCAGG	CATTCA	TCCC	GGT	CAC	TTTG	GGTA	CAGGGGAGCTGGTGGGCAGGGT	7080	
H19-219	6961	AGCTGGGACGATGGGCTGAGCTAGGGC	TGGAAAAGAAGGGGGAGCCAGG	CATTCA	TCCC	GGT	CAC	TTTG	GGTA	CAGGGGAGCTGGTGGGCAGGGT	7080	
H19-220	6961	AGCTGGGACGATGGGCTGAGCTAGGGC	TGGAAAAGAAGGGGGAGCCAGG	CATTCA	TCCC	GGT	CAC	TTTG	GGTA	CAGGGGAGCTGGTGGGCAGGGT	7080	
H19-221	6961										-----	7080
H19-222	6961	AGCTGGGACGATGGGCTGAGCTAGGGC	TGGAAAAGAAGGGGGAGCCAGG	CATTCA	TCCC	GGT	CAC	TTTG	GGTA	CAGGGGAGCTGGTGGGCAGGGT	7080	
H19-223	6961										-----	7080
H19-224	6961	AGCTGGGACGATGGGCTGAGCTAGGGC	TGGAAAAGAAGGGGGAGCCAGG	CATTCA	TCCC	GGT	CAC	TTTG	GGTA	CAGGGGAGCTGGTGGGCAGGGT	7080	
H19-225	6961	AGCTGGGACGATGGGCTGAGCTAGGGC	TGGAAAAGAAGGGGGAGCCAGG	CATTCA	TCCC	GGT	CAC	TTTG	GGTA	CAGGGGAGCTGGTGGGCAGGGT	7080	
H19-226	6961	AGCTGGGACGATGGGCTGAGCTAGGGC	TGGAAAAGAAGGGGGAGCCAGG	CATTCA	TCCC	GGT	CAC	TTTG	GGTA	CAGGGGAGCTGGTGGGCAGGGT	7080	
H19-227	6961	AGCTGGGACGATGGGCTGAGCTAGGGC	TGGAAAAGAAGGGGGAGCCAGG	CATTCA	TCCC	GGT	CAC	TTTG	GGTA	CAGGGGAGCTGGTGGGCAGGGT	7080	
H19-228	6961	AGCTGGGACGATGGGCTGAGCTAGGGC	TGGAAAAGAAGGGGGAGCCAGG	CATTCA	TCCC	GGT	CAC	TTTG	GGTA	CAGGGGAGCTGGTGGGCAGGGT	7080	
H19-229	6961	AGCTGGGACGATGGGCTGAGCTAGGGC	TGGAAAAGAAGGGGGAGCCAGG	CATTCA	TCCC	GGT	CAC	TTTG	GGTA	CAGGGGAGCTGGTGGGCAGGGT	7080	
H19-230	6961	AGCTGGGACGATGGGCTGAGCTAGGGC	TGGAAAAGAAGGGGGAGCCAGG	CATTCA	TCCC	GGT	CAC	TTTG	GGTA	CAGGGGAGCTGGTGGGCAGGGT	7080	
H19-231	6961	AGCTGGGACGATGGGCTGAGCTAGGGC	TGGAAAAGAAGGGGGAGCCAGG	CATTCA	TCCC	GGT	CAC	TTTG	GGTA	CAGGGGAGCTGGTGGGCAGGGT	7080	

Fig 4.17: All Ensembl transcripts except H19-211, 217, 221 and 223 contain the target sequence

4.2 Experimental Validation

As hsa-mir-149-5p is found downregulated in the Meningioma data from AIIMS and in samples with high H19 counts, we hypothesise that the lncRNA H19 sponges the miRNA hsa-mir-149-5p which may be a key contributor to the pathoetiology of Meningioma. We plan to test this assumption in the remainder of the time allotted for the B. Tech Project by preparing an overexpression clone of hsa-mir-149-5p, testing its effects on a gene of interest and performing cell based assays to analyse effects on cancer hallmarks like proliferation, migration and apoptosis.

4.2.1 Primer Design

Five primers were designed for making an overexpression clone of hsa-mir-149-5p and for subsequent detection by RT-qPCR. These are described in Table 4.15.

Table 4.8: Details of cloning and detection primers for hsa-miR-149-5p

SR. NO.	NAME	SEQUENCE (5'-3')	LENGTH	GC% content	TM (Gene Runner)	TM (Thermo Tm Cal)
1	miR149- FP-CP	5' ATCAGGATCCCG CAGAAGGAAGGCCAG 3'	26 bp	57.69%	71.5	68.8
2	miR149- RP-CP	5' ATTAGAATTCCGTA AGATATGGGAGCTCC 3'	29 bp	41.38%	63.6	61.7
3	miR149- 5p-Stem Loop-RT	5'GTCGTATCCAGTGCAG GTCCGAGGTATTCGCACT GGATACGACGGGAGT 3'	50 bp	58.00%	86.2	77.4
4	miR149- 5pFP- QPCR	5' TAGCTCTGGCTCCG TGTCTTC 3'	21 bp	57.10%	59.4	63.1
5	UnivRev P-QPCR	5' GTGCAGGGTCC GAGGTATTC 3'	20 bp	60.00%	59.2	60.1

4.2.2 Preparation of Overexpression Construct of miR-149

The overexpression construct for miR-149 was successfully prepared.

4.2.2.1 Temperature Standardisation of Cloning Primers

Temperature standardisation of the primers was a major time-limiting step in undertaking experimental validation. The experiment had to be repeated multiple times with different combinations of reagents to obtain a successful amplicon and identify an optimum temperature. We discovered that initial experiments failed due to a DNase contamination in the batch of PCR water used for the PCR reaction and for preparing the primer dilutions. The PCR water was replaced but only very thin bands were obtained from IOMM Lee cells. We obtained significant amplification by replacing the HF buffer with GC buffer and increasing the initial denaturation time. This may be due to the high GC content in the template genomic DNA responsible for transcribing miR-149. The reaction was found to be nonspecific at low temperatures and gave a variety of products, none of which were close to miR-149 in length (408bp). Specificity increases with temperature and the ideal amplification temperature is 62°C. These results are shown in Fig 4.18.

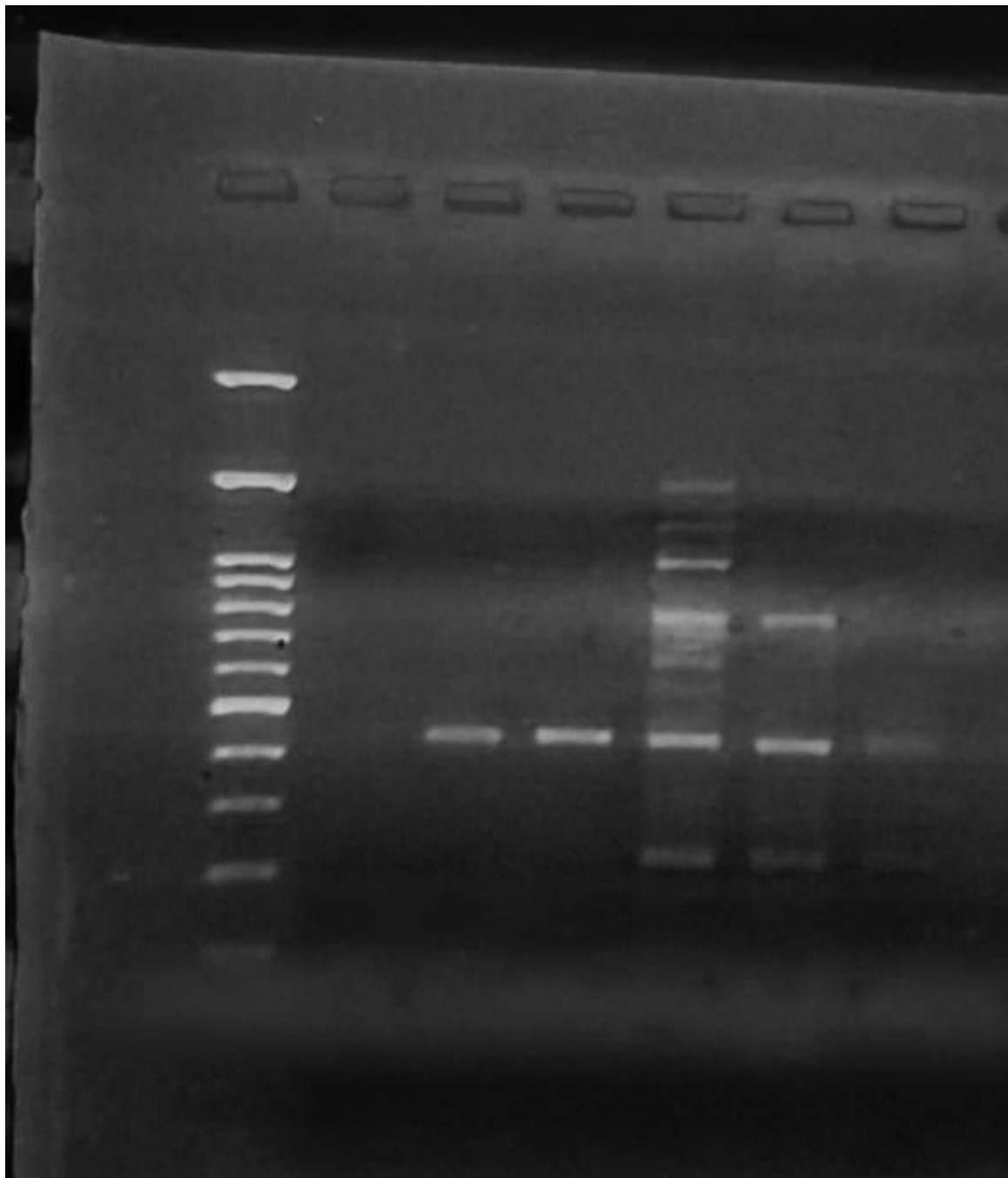


Fig 4.18: PCR amplification results at different temperatures. First well: 100bp ladder, second well: reaction at 64°C, third well: reaction at 62°C, fourth well: reaction at 60°C, fifth well: reaction at 58°C, sixth well: reaction at 56°C, seventh well: reaction at 54°C

4.2.2.2 PCR Amplification

The use of GC buffer gave clear bright bands at 408bp, indicating significant amplification of miR-149.

4.2.2.3 Gel Elution

The amplified DNA was eluted from the gel into 2 microcentrifuge tubes (MCTs) labelled I and II. These were analysed on Nanodrop for purity and for use in further calculations.

Table 4.9: Nanodrop analysis of DNA eluted from gel

Sample	Quantity (ng/ μ L)	A 260/280	A 260/230
I	16.9	2.05	0.02
II	13.9	2.11	0.02

4.2.2.3 Restriction Enzyme Digestion

The insert and plasmid were successfully digested with EcoRI and BamHI as shown in Fig 4.19. The band in the first well indicates the presence of linearised plasmid pcDNA 3.1+. The second well shows uncut pcDNA 3.1(+) plasmid. The band in the third well is at ~400 bp and indicates successful digestion of the miR-149 amplicon which will serve as our insert.

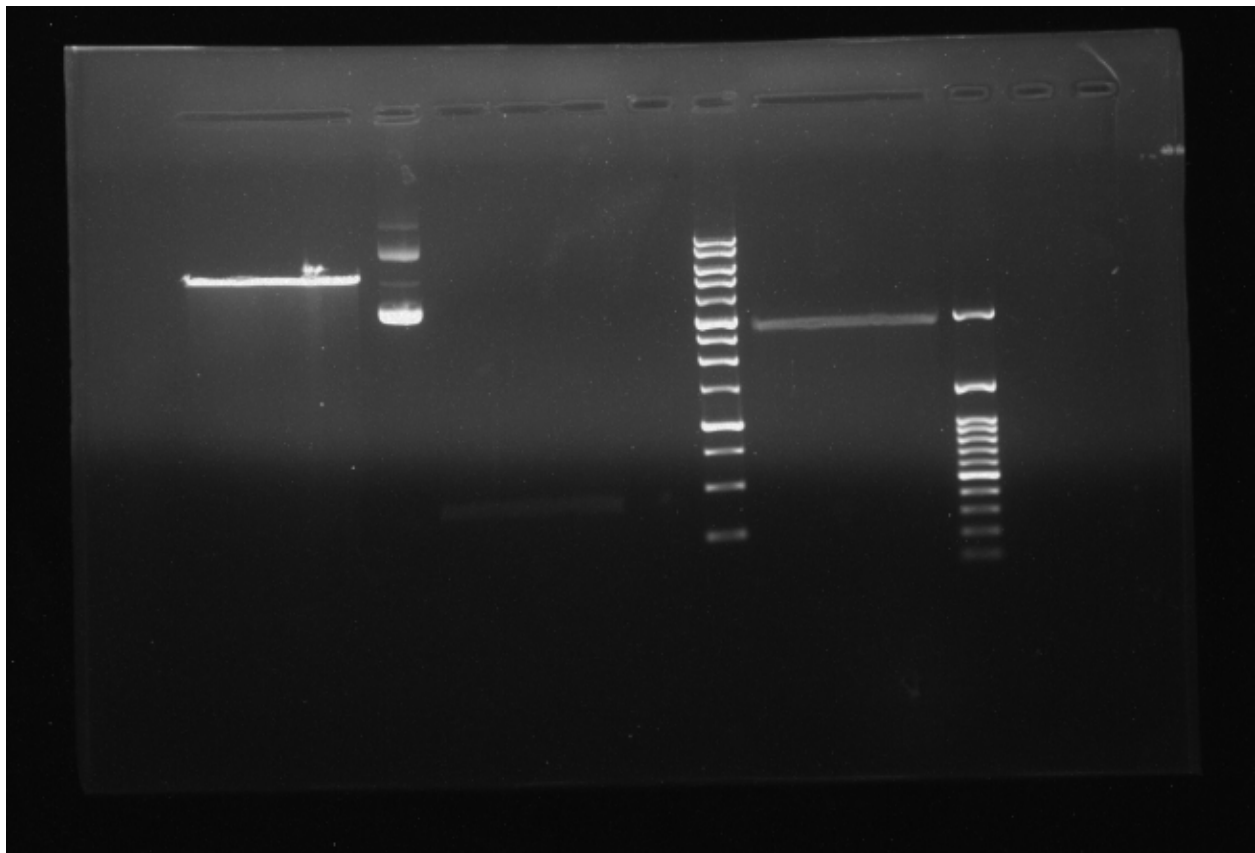


Fig 4.19: Agarose gel analysis of restriction enzyme digestion. Well 1: cut plasmid, Well 2: uncut plasmid, Well 3: cut miR 149 insert, Well 4: 1kb ladder, Well 5: cut H19 insert, Well 6: 100bp ladder.

4.2.2.4 Ligation

The ligation reaction was carried out overnight at 4°C.

4.2.2.5 Transformation

The ligation mixture was successfully transformed into *E. coli*. As shown in Fig 4.20, many colonies were obtained on both plates A and B in the presence of the selection marker Ampicillin.

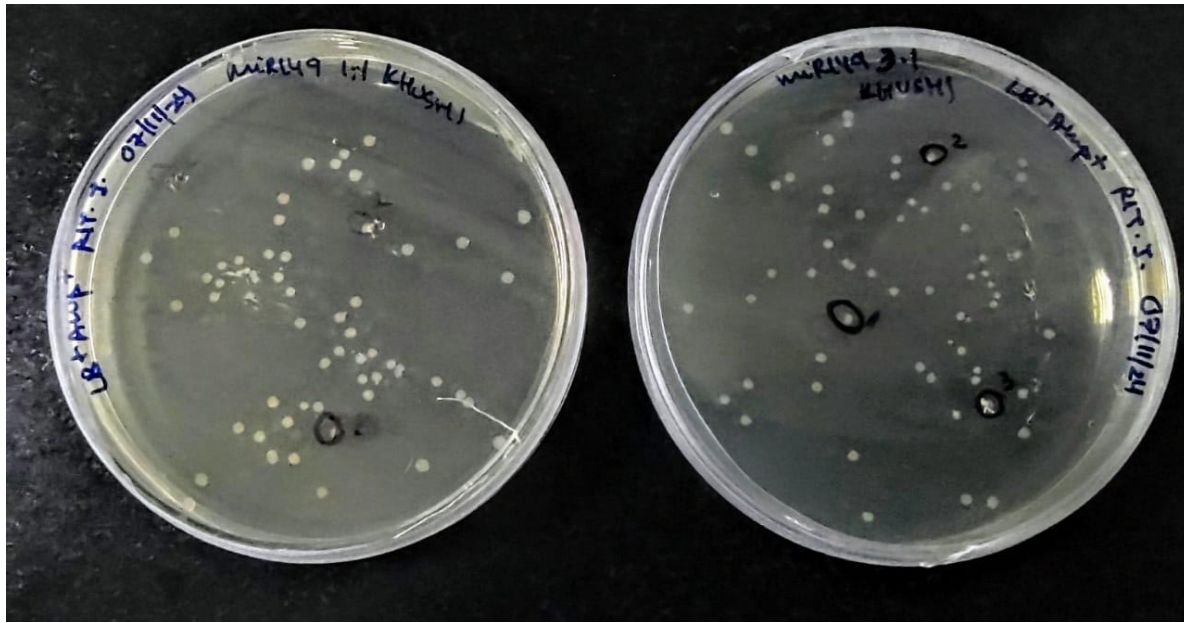


Fig 4.20: Colonies obtained after transformation with pcDNA 3.1+ and miR-149 ligation mixtures

4.2.2.6 Validation of presence of miR-149 insert in colonies

While the presence of colonies on the Ampicillin plate confirms the presence of vectors in the colony, it does not give any information on the presence of the insert. The plate would contain two types of colonies - colonies containing self ligated vector and colonies with ligated vector and insert. Further validation is required to confirm the presence of insert.

4.2.2.6.1 Colony PCR

Colony PCR was positive for the insert for all colonies tested. Bands at 408 bp were observed from all colonies. This indicates the presence of miR-149 insert. These colonies were used to start primary cultures.

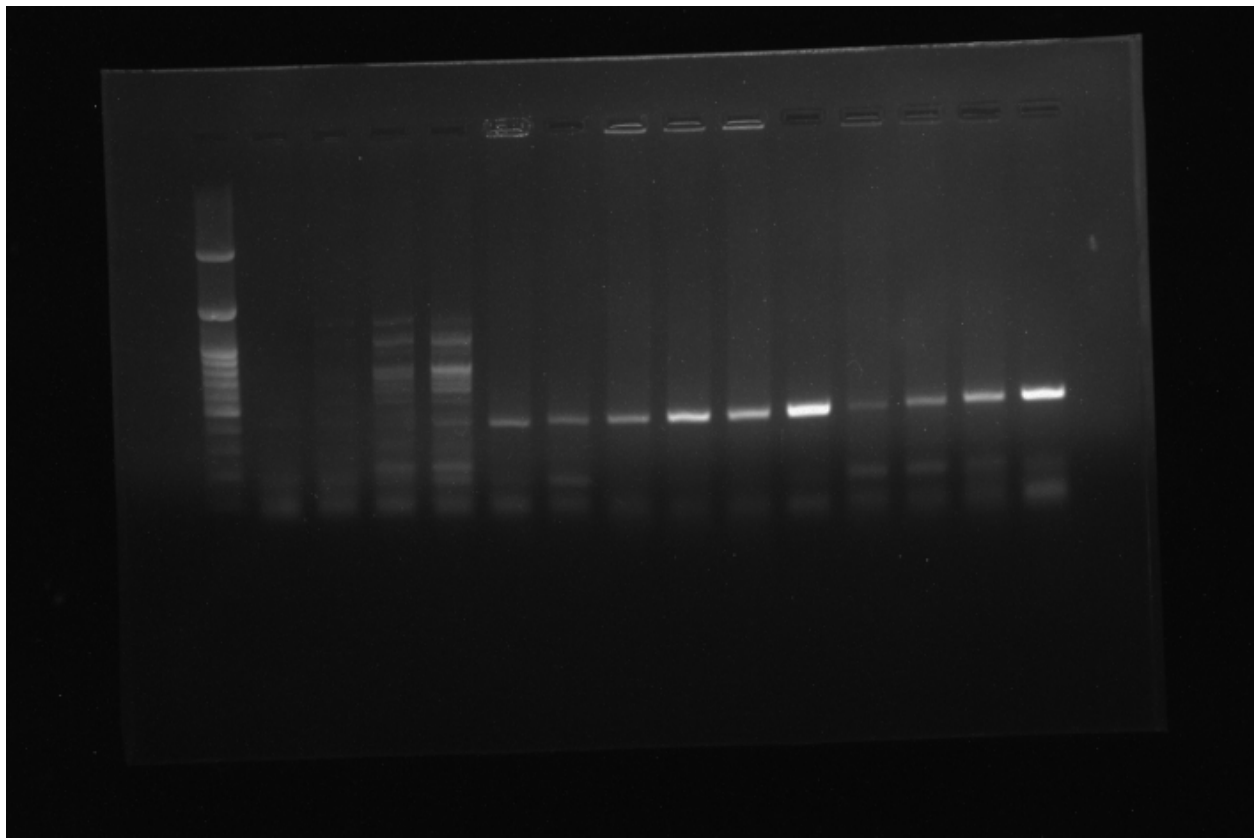


Fig 4.19: Results of colony PCR. Well 1: 100 bp ladder, other wells- colony PCR amplicons

4.2.2.6.2 Plasmid Extraction and Digestion

The plasmids extracted from chosen colonies were found positive for the presence of miR-149 insert after digestion with EcoRI and BamHI. This further confirms the presence of the insert in our clone.

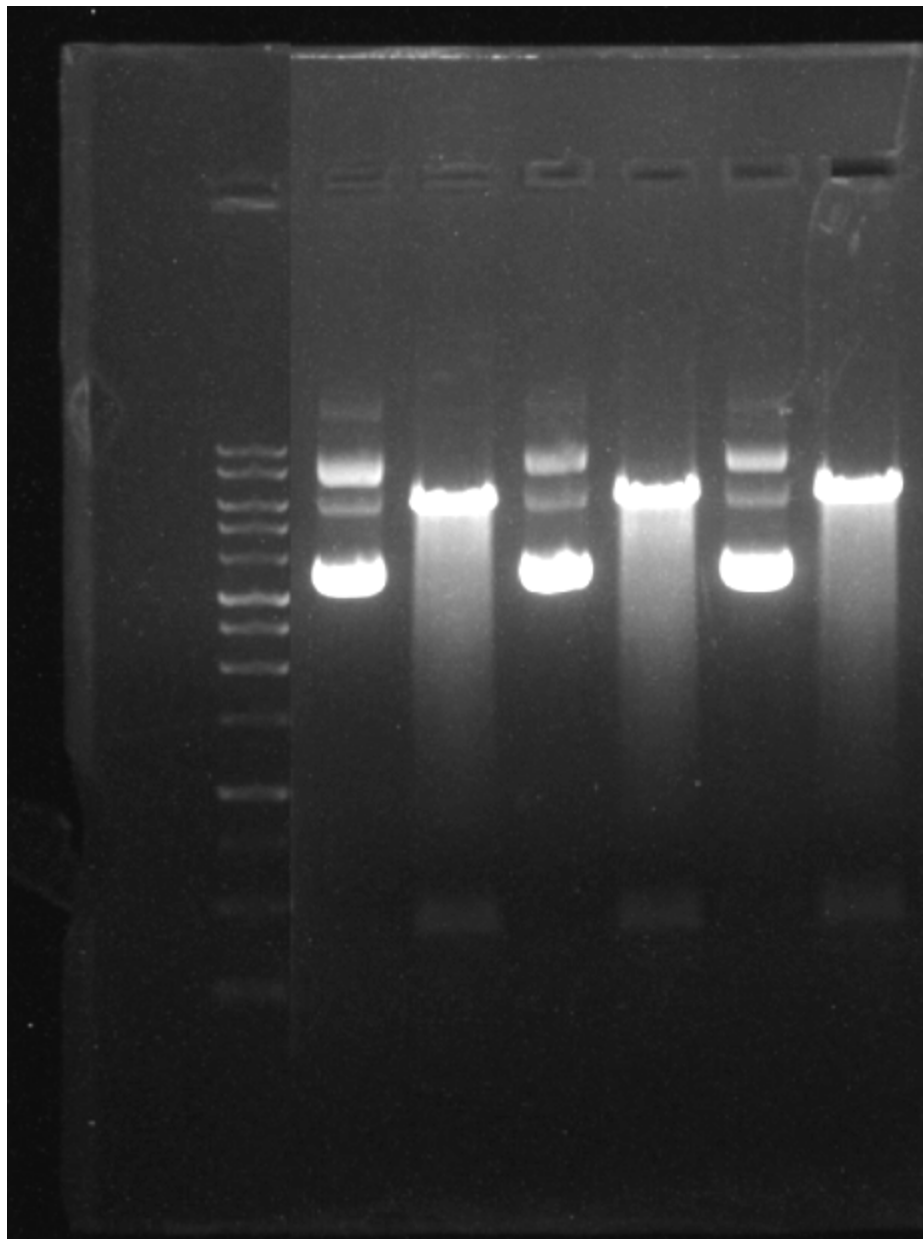


Fig 4.20: Results of restriction digestion of plasmids extracted from colonies chosen after colony PCR. Well 1: 100 bp ladder, Well 2: digested colony 1 plasmid, Well 3: undigested colony 1 plasmid, Well 4: digested colony 2 plasmid, Well 5: undigested colony 2 plasmid, Well 6: digested colony 3 plasmid, Well 7: undigested colony 3 plasmid

4.2.2.6.3 Sequencing

For final verification of the clone, we await the results of Sanger sequencing.

Summary and Conclusions

In conclusion, we have performed a thorough bioinformatic analysis of the differential gene expression w.r.t H19 data for Meningioma patients. We have investigated the results from the perspectives of gene ontology, cellular pathways, role in cancer, immune infiltration, coexpression analysis, protein-protein interaction and ceRNA interactions. Our results established initial validation for the core hypothesis of the umbrella project, concerning the key role of the long non-coding RNA H19 in Meningioma. ceRNA analysis yielded the most interesting results, which led directly to our candidate miRNA to be targeted in this B. Tech. project- **hsa-miR-149-5p**. This is a very promising target by virtue of its implication in a wide variety of other cancers, including other CNS cancers and spanning every major organ system of the body. The novelty aspect is provided by the lack of research on the role of this miRNA in Meningioma. The miR-149 overexpression clone thus obtained may be used to perform functional analysis to identify the role of miR-149 in meningioma. The ceRNA association of H19 and miR-149 may be confirmed indirectly (via RT-qPCR upon modulation of the expression levels of either miR-149 or H19) and directly (Dual Luciferase Assay and Ago-based RNA IP).

Chapter X

References

1. World Health Organisation. The Top 10 Causes of Death.
<https://www.who.int/news-room/fact-sheets/detail/the-top-10-causes-of-death> (2024).
2. National Cancer Institute (NCI). Cancer Statistics.
https://www.google.com/url?q=https://www.cancer.gov/about-cancer/understanding/statistics&sa=D&source=docs&ust=1727008096561167&usg=AOvVaw2zKaOcYACIr3s6_30x_uPd (2024).
3. Buerki, R. A. *et al.* An overview of meningiomas. *Future Oncol. Lond. Engl.* **14**, 2161–2177 (2018).
4. Alruwaili AA, D. J. O. *Meningioma*. (StatPearls Publishing, 23 08 23).
5. Hargadon, K. M. Genetic dysregulation of immunologic and oncogenic signaling pathways associated with tumor-intrinsic immune resistance: a molecular basis for combination targeted therapy-immunotherapy for cancer. *Cell. Mol. Life Sci.* **80**, 40 (2023).
6. Casamassimi, A., Federico, A., Rienzo, M., Esposito, S. & Ciccodicola, A. Transcriptome Profiling in Human Diseases: New Advances and Perspectives. *Int. J. Mol. Sci.* **18**, 1652 (2017).
7. Salmena, L., Poliseno, L., Tay, Y., Kats, L. & Pandolfi, P. P. A ceRNA Hypothesis: The Rosetta Stone of a Hidden RNA Language? *Cell* **146**, 353–358 (2011).
8. Yang, N., Liu, K., Yang, M. & Gao, X. ceRNAs in Cancer: Mechanism and Functions in a Comprehensive Regulatory Network. *J. Oncol.* **2021**, 4279039 (2021).
9. Connolly, I. D. *et al.* Craniotomy for Resection of Meningioma: An Age-Stratified Analysis of the MarketScan Longitudinal Database. *World Neurosurg.* **84**, 1864–1870 (2015).
10. Backer-Grøndahl, T., Moen, B. H. & Torp, S. H. The histopathological spectrum of human meningiomas. *Int. J. Clin. Exp. Pathol.* **5**, 231–242 (2012).

11. Zhao, L. *et al.* An Overview of Managements in Meningiomas. *Front. Oncol.* **10**, 1523 (2020).
12. Caruso, G. *et al.* Novel Advances in Treatment of Meningiomas: Prognostic and Therapeutic Implications. *Cancers* **15**, 4521 (2023).
13. Eraky, A. M. Non-coding RNAs as Genetic Biomarkers for the Diagnosis, Prognosis, Radiosensitivity, and Histopathologic Grade of Meningioma. *Cureus* **15**, e34593 (2023).
14. Yang, J., Qi, M., Fei, X., Wang, X. & Wang, K. LncRNA H19: A novel oncogene in multiple cancers. *Int. J. Biol. Sci.* **17**, 3188–3208 (2021).
15. Li, Y. *et al.* LncRNA H19 promotes triple-negative breast cancer cells invasion and metastasis through the p53/TNFAIP8 pathway. *Cancer Cell Int.* **20**, 200 (2020).
16. Zhang, X. *et al.* The role of lncRNA H19 in tumorigenesis and drug resistance of human Cancers. *Front. Genet.* **13**, 1005522 (2022).
17. Uhlmann, E. J. *et al.* Inhibition of the epigenetically activated miR-483-5p/IGF-2 pathway results in rapid loss of meningioma tumor cell viability. *J. Neurooncol.* **162**, 109–118 (2023).
18. Love, M. I., Huber, W. & Anders, S. Moderated estimation of fold change and dispersion for RNA-seq data with DESeq2. *Genome Biol.* **15**, 550 (2014).
19. Clough, E. & Barrett, T. The Gene Expression Omnibus Database. *Methods Mol. Biol. Clifton NJ* **1418**, 93–110 (2016).
20. Kuleshov, M. V. *et al.* Enrichr: a comprehensive gene set enrichment analysis web server 2016 update. *Nucleic Acids Res.* **44**, W90-97 (2016).
21. Kanehisa, M., Furumichi, M., Tanabe, M., Sato, Y. & Morishima, K. KEGG: new perspectives on genomes, pathways, diseases and drugs. *Nucleic Acids Res.* **45**, D353–D361 (2017).
22. Li, G. *et al.* Long non-coding RNA-H19 stimulates osteogenic differentiation of bone marrow mesenchymal stem cells via the microRNA-149/ SDF-1 axis. *J. Cell. Mol. Med.* **24**, 4944–4955 (2020).

23. Huang, W. *et al.* Regulatory mechanism of miR-20a-5p expression in Cancer. *Cell Death Discov.* **8**, 262 (2022).
24. Khalilian, S., Abedinlou, H., Hussen, B. M., Imani, S. Z. H. & Ghafouri-Fard, S. The emerging role of miR-20b in human cancer and other disorders: Pathophysiology and therapeutic implications. *Front. Oncol.* **12**, 985457 (2022).
25. Liu, H. & Wang, G. MicroRNA-301a-3p promotes triple-negative breast cancer progression through downregulating MEOX2. *Exp. Ther. Med.* **22**, 945 (2021).
26. Zhang, J. *et al.* Hsa-miR-301a-3p inhibited the killing effect of natural killer cells on non-small cell lung cancer cells by regulating RUNX3. *Cancer Biomark. Sect. Dis. Markers* **37**, 249–259 (2023).
27. Ren, F.-J. *et al.* MiR-149-5p: An Important miRNA Regulated by Competing Endogenous RNAs in Diverse Human Cancers. *Front. Oncol.* **11**, 743077 (2021).
28. Liu, L. *et al.* CircGPR137B/miR-4739/FTO feedback loop suppresses tumorigenesis and metastasis of hepatocellular carcinoma. *Mol. Cancer* **21**, 149 (2022).
29. Wang, X. *et al.* ZEB1 activated-VPS9D1-AS1 promotes the tumorigenesis and progression of prostate cancer by sponging miR-4739 to upregulate MEF2D. *Biomed. Pharmacother. Biomedecine Pharmacother.* **122**, 109557 (2020).

Chapter XX
Supplementary

Table S1: Top 20 biological processes enriched in association with upregulated DEGs

Biological Process	Adjusted p value	Upregulated Genes
Microtubule Cytoskeleton Organization Involved In Mitosis	1.24E-06	ESPL1;KIF4A;NUF2;NUSAP1;CDK1;BIRC5;KIF11;DLGAP5;AURKB;SPC25
Mitotic Sister Chromatid Segregation	2.67E-06	KIF18A;KIF18B;ESPL1;CDC45;CENPK;NUSAP1;KIF14;NCAPG;KIF11;NCAPH;CEP55;DLGAP5
Spindle Assembly Checkpoint Signalling	2.85E-06	CENPF;NUF2;BUB1B;TRIP13;BUB1;SPC24;SPC25
Mitotic Spindle Assembly Checkpoint Signalling	2.85E-06	CENPF;NUF2;BUB1B;TRIP13;BUB1;SPC24;SPC25
Mitotic Spindle Checkpoint Signalling	2.85E-06	CENPF;NUF2;BUB1B;TRIP13;BUB1;SPC24;SPC25
Negative Regulation Of Mitotic Metaphase/Anaphase Transition	4.19E-06	CENPF;NUF2;BUB1B;TRIP13;BUB1;SPC24;SPC25
Positive Regulation Of Mitotic Sister Chromatid Separation	8.65E-05	ESPL1;UBE2C;BIRC5;AURKB;DLGAP5
Positive Regulation Of Cell Cycle Process	1.36E-04	NUSAP1;KIF14;NCAPG;BIRC5;CDC6;NCAPH;AURKB;E2F7;AURKA;E2F8
Sister Chromatid Segregation	2.49E-04	TOP2A;KIF18A;KIF18B;ESPL1;CENPK;NUSAP1

Negative Regulation Of Cell Cycle Process	2.49E-04	ESPL1;NEK2;FBXO43;AURKB;E2F7;E2F8
Mitotic Cytokinesis	4.92E-04	ESPL1;KIF4A;NUSAP1;BIRC5;CENPA;CEP55;AURKB
Mitotic Spindle Organization	5.36E-04	KIF4A;NUF2;BIRC5;KIF11;DLGAP5;AURKB;AURKA;SPC25
Mitotic Nuclear Division	0.001046	KIF18A;KIF18B;ESPL1;UBE2C;CENPK;NUSAP1
Regulation Of Chromosome Segregation	0.001258	NCAPG;CDC6;MKI67;BUB1;NCAPH
Antimicrobial Humoral Response	0.001438	COLEC11;GNLY;S100A12;DEFA3;PRTN3;RNASE3;PI3;DEFA1
Mitotic Chromosome Condensation	0.001569	CDCA5;NUSAP1;NCAPG;NCAPH
Metaphase Plate Congression	0.001673	CENPF;KIF18A;CDCA5;KIF14;FAM83D;CEP55
Chromosome Condensation	0.001935	TOP2A;CDCA5;NUSAP1;NCAPG;NCAPH
Cytoskeleton-Dependent Cytokinesis	0.002361	ESPL1;KIF4A;NUSAP1;BIRC5;CENPA;CEP55;AURKB
Striated Muscle Contraction	0.002385	MYL4;CSRP3;TNNT2;TNNT3;TNNI1;TNI3

Table S2: Biological processes significantly enriched in association with downregulated DEGs

Biological Process	Adjusted p value	Downregulated Genes
Modulation Of Chemical Synaptic Transmission	0.0042899	RIMS2;SLC4A8;CLSTN2;NRG3;GRIK3;DLGAP1;NPTXR;SYN3;CPLX1;GRIA3
Chemical Synaptic Transmission	0.0058677	NPY5R;STXBP1;GRIK3;SLC1A2;LIN7A;SYN3;CPLX1;HTR6;PTCHD1;CDHR3;SNCG;DLGAP1;AMPH;GRIA3
Negative Regulation Of Monoatomic Ion Transport	0.0273566	CASQ2;STC1;VIP;ADRA2A
Positive Regulation Of Excitatory Postsynaptic Potential	0.0471638	RIMS2;CUX2;PRKCZ;SHANK1
Neurotransmitter Secretion	0.0493215	RIMS2;STXBP1;LIN7A;SYN3;CPLX1

TableS3: Molecular functions the products of the upregulated DEGs are implicated in

Molecular Function	Adjusted p value	Upregulated Genes
Microtubule Binding	0.003155264	KIF18A;KIF18B;KIF14;NUSAP1;BIRC5;FAM83D;GTSE1;SKA1;DLGAP5;SPC24;S100A8;KIF15
Tubulin Binding	0.027187154	KIF18A;KIF18B;KIF14;NUSAP1;BIRC5;FAM83D;GTSE1;SKA1;DLGAP5;SPC24;S100A8;KIF15

Table S4: Molecular functions the products of the downregulated DEGs are implicated in

Molecular Function	Adjusted p value	Upregulated Genes
Sodium-Independent Organic Anion Transmembrane Transporter Activity	0.008276111	SLCO1C1;SLC22A6;SLCO1A2;SLC O2A1
Potassium Channel Activity	0.008296416	KCNT1;KCND3;KCNS2;KCNA2;GR IK3;KCNK2;HCN1
Outward Rectifier Potassium Channel Activity	0.020588797	KCNT1;KCND3;KCNK2
Voltage-Gated Potassium Channel Activity	0.035149106	KCNT1;KCND3;KCNJ9;KCNS2;KC NA2;KCNK2
Low-Density Lipoprotein Particle Binding	0.048483438	COLEC12;SCARB1;PLTP
Neuropeptide Receptor Activity	0.048483438	NPFFR1;NPY5R;NPY1R;SSTR1

Table S5: Cellular components overrepresented in association with upregulated DEGs

Cellular Component	Adjusted p value	Upregulated Genes
Mitotic Spindle	8.76E-07	CKAP2L;CDC6;KIF11;SKA1;AURKA;KI F18A;KIF18B;ESPL1;NUSAP1;CDK1;M YF6;FAM83D;DLGAP5
Spindle	8.76E-07	CKAP2L;BUB1B;CDC6;KIF11;SKA1;A URKB;AURKA;CENPF;ESPL1;KIF4A;N USAP1;CDK1;MYF6;FAM83D;DLGAP5
Spindle Microtubule	3.59E-05	KIF18A;KIF18B;KIF4A;CDK1;KIF11;A URKB;SKA1;AURKA
Microtubule Cytoskeleton	2.22E-04	CKAP2L;KIF14;BUB1B;KIF11;SKA1;A URKB;KIF15;AURKA;CCNB2;CENPF;K IF18A;BIRC5;FAM83D;GTSE1;TRIM55

Secretory Granule Lumen	0.001417009	FCN1;FGG;DEFA3;RNASE3;DEFA1;OLFM4;MMP8;TCN1;S100A12;PRTN3;ELANE;S100A8;SGCG
Microtubule	0.004891822	KIF4A;CDK1;KIF14;KIF11;SKA1;TRIM55;AURKB;KIF15;AURKA
Chromosome	0.0091423	TOP2A;BLM;CDCA5;NCAPG;BIRC5;ESCO2;TRIP13;MKI67
Nuclear Chromosome	0.010603443	TOP2A;BLM;CDC45;BIRC5;NCAPG;NCAPH
Keratin Filament	0.01264495	KRT17;KRT16;KRT14;KRT9
Intermediate Filament	0.012910718	KRT17;KRT16;KRT14;KRT9;GFAP
Astral Microtubule	0.020626724	KIF18A;KIF18B
Intermediate Filament Cytoskeleton	0.02203455	KRT17;KRT16;KRT14;S100A8;GFAP
Sarcolemma	0.02575388	TRIM72;CAV1;CACNG1;SGCG
Azurophil Granule Lumen	0.028491791	DEFA3;PRTN3;RNASE3;DEFA1;ELANE
Myofibril	0.033114041	MYH2;TNNT2;TNNI3
Nucleus	0.033114041	TOP2A;ARHGAP11A;MCM10;KIF11;MKI67;HOXA11;CSRP3;EXO1;ANKRD1;PBK;C16ORF78;NEK2;MYBL2;PITX1;DLGAP5;MYOG;DUSP2;SOX11;ESCO2;TEX15;IGFN1;KRT9;RIPPLY1;C15ORF48;ASPM;MYH2;ESPL1;DPPA4;BIRC5;HOBXB7;PRR11;ROPN1;S100A8;HOBXB5;ACTRT1;BLM;CEBPE;CDCA5;NCAPG;FBXO43;CENPA;AURKB;AURKA;STRA8;CCNB2;CDC45;UBE2NL;IGF2BP1;S100A12;HOXC4;PMAIP1;IGF2BP3;NKX2-5;CDKN2A;UBE2C;CDC6;GADD45G;FA

		M111B;CENPF;KIF18A;KIF18B;DIAPH3;KRT16;KRT14;MYF6;CDK1;TRIP13
Condensed Chromosome	0.033114041	NCAPG;MKI67;CENPA;NCAPH
Specific Granule Lumen	0.03318283	TCN1;MMP8;OLFM4;ELANE
Serine-Type Endopeptidase Complex	0.034791114	FCN1;COLEC11
Cytoskeleton	0.0429055	CKAP2L;SKA1;AURKB;GFAP;AURKA;CCNB2;KIF18A;KRT17;KRT16;S100A12;BIRC5;FAM83D;GTSE1;S100A8
Intracellular Non-Membrane-Bounded Organelle	0.0429055	TOP2A;BLM;CDCA5;CAV1;HJURP;BU B1B;MCM10;ESCO2;CDC6;KIF11;MKI6 7;AURKB;AURKA;CENPF;KRT16;NUS AP1;S100A12;IGF2BP3;TRIP13;FAM83 D;SPC24;S100A8;E2F8
Serine-Type Peptidase Complex	0.0429055	FCN1;COLEC11
Azurophil Granule	0.0429055	DEFA3;PRTN3;RNASE3;DEFA1;OLFM4 ;ELANE
Specific Granule	0.045317629	MS4A3;TCN1;OLFM4;MMP8;LILRA3;ELANE
Collagen-Containing Extracellular Matrix	0.045317629	FCN1;TNXB;FGG;PRTN3;LAMC2;CLC;DEFA1;MMP8;ELANE;S100A8
Vacuolar Lumen	0.045317629	GPC3;DEFA3;PRTN3;RNASE3;DEFA1;ELANE
Polymeric Cytoskeletal Fiber	0.045743335	DIAPH3;KRT16;KRT14;KIF14;KIF11;TRIM55;KIF15;GFAP
Endopeptidase Complex	0.046367682	FCN1;COLEC11

Table S6: Cellular components overrepresented in association with downregulated DEGs

Cellular Component	Adjusted p value	Downregulated Genes
Neuron Projection	2.51E-07	GPM6A;CNTNAP2;ADCYAP1R1;KCNA2;GRIK3;STMN4;KNDC1;HTR6;APOD;NCDN;RGS6;EPHA5;SYT4;PACRG;EPHA6;NPY5R;NPY1R;SSTR1;SYT7;NELL2;SLC4A8;NFASC;ALDH1A1;RGS7B P;VIP;SHANK1;HCN1
Dendrite	0.002480561	EPHA5;CNTNAP2;EPHA6;KCNA2;GRIK3;KNDC1;LAMP5;SLC4A8;HTR6;APOD;NCDN;SHANK1 ;HCN1
Axon	0.002505337	EPHA5;NELL2;SYT4;CNTNAP2;NFASC;KCNA2;ALDH1A1;GRIK3;NCDN;SYT7;HCN1
Basolateral Plasma Membrane	0.010305582	SLCO1C1;SLC14A1;SLC22A6;SLC13A3;CA4;SLC6A13;AQP4;LIN7A;ADRA2A
Glutamatergic Synapse	0.011352636	NELL2;SLC4A8;NRG3;DLGAP1;NPTXR;SHISA7
Glial Cell Projection	0.011352636	SLC4A8;SLC1A2;ATP1B2
Voltage-Gated Potassium Channel Complex	0.042428357	CNTNAP2;KCND3;KCNS2;KCNA2;HCN1

Table S7: Pathways in which the upregulated DEGs are significantly implicated.

Pathway	Adjusted p value	Upregulated Genes
Cell cycle	1.46E-04	CCNB2;ORC6;CDC45;ESPL1;CDKN2A; CDK1;BUB1B;CDC6;BUB1;GADD45G
p53 signalling pathway	9.59E-04	CCNB2;RRM2;CDKN2A;CDK1;PMAIP1; GTSE1;GADD45G
Staphylococcus aureus infection	0.003527003	KRT17;KRT16;FGG;KRT14;DEFA3; DEFA1;KRT9

Table S8: Pathways in which the downregulated DEGs are significantly implicated.

Pathway	Adjusted p value	Downregulated Genes
Neuroactive ligand-receptor interaction	4.24E-03	PTGFR;ADCYAP1R1;NPFFR1;NPY5R;PTGER3;GRIK3;NPY1R;SSTR1;AGT;MCHR2; ADRA2A;HTR6;EDNRB;VIP;GRIA3
cAMP signalling pathway	0.031621672	HTR6;ADCYAP1R1;PPP1R1B;PTGER3;NPY1R;ATP1B2;SSTR1;VIP;GRIA3;RAPGEF4